

# Influence of CO<sub>2</sub> adsorption on cylinders and fractionation of CO<sub>2</sub> and air during preparation of a standard mixture

Nobuyuki Aoki<sup>1</sup>, Shigeyuki Ishido<sup>2</sup>, Shohei Murayama<sup>2</sup>, and Nobuhiro Matsumoto<sup>1</sup>

<sup>1</sup>National Metrology Institute of Japan, National Institute of Advanced Industrial Science and Technology (NMIJ/AIST), 1-1-1 Umezono, Tsukuba 305-8563, Japan

<sup>2</sup>Environmental Management Research Institute, National Institute of Advanced Industrial Science and Technology (EMRI/AIST), Tsukuba 305-8569, Japan

*Correspondence to:* Nobuyuki Aoki ([aoki-nobu@aist.go.jp](mailto:aoki-nobu@aist.go.jp)) Tel: +81-29-861-6824; fax: +81-29-861-6854.

**Abstract:** We conducted a study to evaluate carbon dioxide (CO<sub>2</sub>) adsorption on a cylinder's internal surface and fractionation of CO<sub>2</sub> and air during the preparation of standard mixtures of atmospheric CO<sub>2</sub> levels through a multistep dilution. It became clear that the CO<sub>2</sub> molar fractions in standard mixtures prepared by diluting pure CO<sub>2</sub> with air three times deviated by  $-0.207 \pm 0.060 \mu\text{mol mol}^{-1}$  on average from the gravimetric values. It indicates that the deviation is larger than a compatibility goal of  $0.1 \mu\text{mol mol}^{-1}$ , which has been recommended by the World Meteorological Organization (WMO). The deviation was consistent with those calculated from two fractionation factors of  $0.99968 \pm 0.00010$  and  $0.99975 \pm 0.00004$ ; one was estimated by mother–daughter transfer experiment that transfer CO<sub>2</sub>/air mixtures from a cylinder to another evacuated receiving cylinder and another was computed by applying the Rayleigh model to the increase in CO<sub>2</sub> molar fractions in a source gas as its pressure depleted from 11.5 MPa to 1.1 MPa. Both fractionation factors also agree within their uncertainties. Additionally, the mother–daughter transfer experiments shows that the deviation is caused by the fractionation of CO<sub>2</sub> and air in the process of transferring a source gas (a CO<sub>2</sub>/air mixture with a higher CO<sub>2</sub> molar fraction than that in the prepared gas mixture). The fact that the CO<sub>2</sub> fractionation effect was less significant when the transfer speed decreased less than  $3 \text{ L min}^{-1}$  suggested that the main factor of the fractionation could be thermal diffusion. Experiments were conducted that a CO<sub>2</sub> in air mixture (CO<sub>2</sub>/Air mixture) was emitted from a cylinder to evaluate the CO<sub>2</sub> adsorption to the internal surface of the cylinder. When the cylinder pressure was reduced

from 11.0 to 0.1 MPa, the CO<sub>2</sub> molar fractions in the mixture stream exiting the cylinder increased by 0.16 ± 0.04 μmol mol<sup>-1</sup>. By applying the Langmuir adsorption-desorption model to the measured data, the amount of CO<sub>2</sub> adsorbed on the internal surfaces of a 10 L aluminum cylinder when preparing a standard mixture with atmospheric CO<sub>2</sub> level was estimated to be 0.027 ± 0.004 μmol mol<sup>-1</sup> at 11.0 MPa.

**Keywords:** standard mixture, atmospheric CO<sub>2</sub>, gravimetric method, fractionation

## 1 Introduction

Carbon dioxide (CO<sub>2</sub>) is an important greenhouse gas that contributes significantly to the radiative forcing of the atmosphere. Numerous laboratories conduct systematic measurements of atmospheric CO<sub>2</sub> to better understand its sources and sinks. The measurements are typically performed using analyzers calibrated by working standards traceable to the CO<sub>2</sub> scale of the World Meteorological Organization (WMO). The WMO has recommended a compatibility goal of 0.1 μmol mol<sup>-1</sup> for CO<sub>2</sub> measurements based on the WMO CO<sub>2</sub> scale in the Northern Hemisphere (WMO, 2019) to address small and globally significant gradients over large spatial scales. The WMO CO<sub>2</sub> scale has been determined only by standard gas mixtures prepared using manometry. It is necessary to validate by standard mixtures prepared using other method such as gravimetry to make the scale more robust. However, the scale of standard mixtures prepared by gravimetry are not consistent among respective laboratories (Tsuboi et al., 2017, Flores et al., 2019), preventing the WMO CO<sub>2</sub> scale to precisely validate.

Recently, several studies have shown that CO<sub>2</sub> adsorbed on the internal surface of a high-pressure cylinder and desorbed from the surface, as the internal pressure decreases (Langenfels et al., 2005, Leuenberger et al., 2015, Brewer et al., 2018, Schibig et al., 2018, Hall et al., 2019). These studies also provided a method to determine the amount of CO<sub>2</sub> adsorbed on the internal surface of a cylinder using a “decanting” experiment to continuously measure the CO<sub>2</sub> molar fraction in a CO<sub>2</sub> in air mixture (CO<sub>2</sub>/air mixture) exiting a cylinder. For example, Leuenberger et al. (2015) estimated the amount of CO<sub>2</sub>, expressed as a fraction of the total gas in a cylinder, to be 0.028 μmol mol<sup>-1</sup> at 6 MPa by applying the Langmuir model (Langmuir, 1918) to the results as 30 L aluminum cylinders were emptied from 6.0 MPa to 0.1 MPa. Schibig

et al (2018) also estimated the amount of CO<sub>2</sub> to be  $0.0165 \pm 0.0016 \mu\text{mol mol}^{-1}$  at 15.0 MPa as 29.5 L aluminum cylinders were emptied from 15.0 MPa to 0.1 MPa. These values cause a small bias in the gravimetrically assigned CO<sub>2</sub> molar fraction in standard mixtures. However, Miller et al. (2015) conducted a series of “mother–daughter” experiments in which they transferred half of a CO<sub>2</sub>/air mixture from a “mother” cylinder into an evacuated “daughter” cylinder. They reported that CO<sub>2</sub> molar fractions in the mother cylinders were 0.02%–0.03% higher than those in the daughter cylinders. The values were greater than the amounts of adsorbed CO<sub>2</sub> estimated by the decanting experiments. According to Hall et al. (2019), CO<sub>2</sub> molar fractions in the mother and daughter cylinders after the mother–daughter experiment were 0.06  $\mu\text{mol mol}^{-1}$  higher and 0.10  $\mu\text{mol mol}^{-1}$ –0.13  $\mu\text{mol mol}^{-1}$  lower, respectively, than CO<sub>2</sub> molar fractions in the mother cylinders before the transfer. The increasing and decreasing amounts were 5 to 10 times larger than the adsorbed amount estimated from their decanting experiments. They proposed that the detected CO<sub>2</sub> change was due to thermal fractionation rather than adsorption of CO<sub>2</sub> on the internal surface of a cylinder. Langenfelds et al. (2005) also assumed diffusive fractionation due to pressure diffusion, thermal diffusion, and effusion were factors that changed CO<sub>2</sub> molar fraction observed in CO<sub>2</sub>/air mixtures due to gas handling. If the CO<sub>2</sub> changes in the transfer are caused by a kinetic process such as the diffusive fractionation, the fractionation factor is considered to be constant regardless of the CO<sub>2</sub> molar fraction. In gravimetry, standard mixtures with atmospheric CO<sub>2</sub> levels are typically prepared through a multistep dilution, which involves diluting pure CO<sub>2</sub> with air two or three times. Each step of dilution is accomplished by transferring a source gas from a “mother” cylinder into an evacuated “daughter” cylinder and pressurizing it with dilution gas air. The fractionation of CO<sub>2</sub> and air (nitrogen, oxygen, argon, and trace impurities other than CO<sub>2</sub>) is likely to occur in the second and third step dilutions because a CO<sub>2</sub>/air mixture with a higher CO<sub>2</sub> molar fraction than that in the prepared standard mixture is used as the source gas. The fractionation process decreases the CO<sub>2</sub> molar fraction in the source gas transferred into the daughter cylinder which causes an increase in the CO<sub>2</sub> molar fraction in the remaining source gas in the mother cylinder because of its consumption. This could be a factor that deteriorates the reproducibility of the assigned CO<sub>2</sub> molar fractions because CO<sub>2</sub> molar fractions in the prepared standard mixtures are biased by the decrease and increase in

CO<sub>2</sub> in the transferred gas mixture and the remaining pre-mixture, respectively. To avoid fractionation in each step dilution, one method is to gravimetrically prepare standard mixtures by one-step dilution to mix pure CO<sub>2</sub> and air directly, as there is no process to transfer a CO<sub>2</sub>/air mixture into another cylinder (Hall et al., 2019). Tohjima et al. (2005) developed a technique to gravimetrically prepare standard mixtures by one-step dilution. However, they did not discuss fractionation and adsorption that occurs during the multistep dilution process.

To accurately determine the CO<sub>2</sub> molar fraction, we must understand the adsorption and fractionation effects on the preparation process of standard mixtures with atmospheric CO<sub>2</sub> levels. Therefore, this study evaluated the systematic error of CO<sub>2</sub> molar fraction in the standard mixtures prepared by multistep dilution and the contribution of its factors. CO<sub>2</sub> adsorption and fractionation are assumed to depend on the type and size of a cylinder (Leuenberger et al, 2015). The evaluation was performed using 10 L aluminum cylinders

which are often used for preparation of gravimetric standard mixtures because previous studies only evaluated CO<sub>2</sub> adsorption and CO<sub>2</sub> and air fractionation in 29.5 L aluminum and 50 L steel cylinders. Based on decanting experiments, we evaluated the amount of CO<sub>2</sub> adsorbed on the internal surface of a 10 L aluminum cylinder. The fractionation of CO<sub>2</sub> and air in the transfer of CO<sub>2</sub>/air mixtures were then evaluated in detail based on mother–daughter experiments using the cylinders, and the fractionation factor in the transfer of a source gas was estimated on the basis of the results. Finally, we demonstrated that standard mixtures gravimetrically prepared by three-step dilutions had a systematic error of CO<sub>2</sub> molar fractions by comparing them with the standard mixtures prepared by one-step dilution.

## 2 Methods

### 2.1 Decanting and mother–daughter experiments

We conducted decanting and mother–daughter experiments to estimate CO<sub>2</sub> adsorption on the internal surface of a cylinder, and the fractionation of CO<sub>2</sub> and air during the transfer of a CO<sub>2</sub>/air mixture into an evacuated cylinder.

The decanting experiments were performed using 10 L aluminum cylinders (Luxfer Gas Cylinders, UK) with a brass diaphragm valve (G-55, Hamai Industries Limited, Japan). The cylinders were evacuated to  $\sim 10^{-4}$  Pa using a turbo molecular pump and pressurized to 11.0 MPa by CO<sub>2</sub>/air mixtures with CO<sub>2</sub> molar fractions ranging from 350  $\mu\text{mol mol}^{-1}$  to 450  $\mu\text{mol mol}^{-1}$ . The CO<sub>2</sub>/air mixtures were decanted using single stage regulators (Torr 1300, NISSAN TANAKA Co., Japan) attached to the cylinders from 11.0 MPa to 0.1 MPa at total flow rates of 80 ml min<sup>-1</sup>, 150 ml min<sup>-1</sup>, and 300 ml min<sup>-1</sup>. After flowing through the regulator, the mixture flow was branched in two ways by T-pieces. The branched flows were controlled by two mass flow controllers (SEC-Z512MGX 100 SCCM, and 1SLM, Horiba STEC Co., Ltd., Japan); one was introduced as sample gas into a Picarro G2301 (Picarro, Inc., USA) at a flow rate of 80 ml min<sup>-1</sup>, and the other was exhausted to the surroundings at rates of 0 ml min<sup>-1</sup>, 70 ml min<sup>-1</sup>, and 220 ml min<sup>-1</sup>. An absolute pressure gauge of flush diaphragm type (PPA-33X, KELLER AG, Switzerland) attached to the regulator was used to measure the pressures in the cylinders. The Picarro G2301 output was linearly calibrated using one standard mixture containing atmospheric CO<sub>2</sub> levels with a standard uncertainty of less than 0.1  $\mu\text{mol mol}^{-1}$  as the signal was assumed to be zero when the CO<sub>2</sub> molar fraction was zero. After calibrating the Picarro G2301 for 20 min, the process of measuring CO<sub>2</sub> in the decanting flow for 100 min was repeated. The decanting flow was stopped while the Picarro G2301 was calibrated using the standard mixture.

The mother–daughter experiment was performed using 10 L or 48 L aluminum cylinders (Luxfer Gas Cylinders, UK) with a brass diaphragm valve. These cylinders were filled with CO<sub>2</sub>/air mixtures with CO<sub>2</sub> molar fractions ranging from 380  $\mu\text{mol mol}^{-1}$  to 460  $\mu\text{mol mol}^{-1}$  and 3.2 MPa to 13.9 MPa; some of these mixtures were purchased from a gas supplier (Japan Fine Products, Japan), while others were prepared at our laboratory. The CO<sub>2</sub>/air mixtures were prepared using pure CO<sub>2</sub> and purified air which was removed from ambient air. In this experiment, the cylinders containing the mixtures were referred to as the mother cylinder, while the receiving cylinders into which the mixture was transferred were referred to as the daughter cylinder. The mixtures in the mother cylinders with vertical or horizontal placements were transferred into the evacuated daughter cylinder with vertical placement through a

manifold made of a 1/4-inch o.d. stainless steel line, diaphragm valves (FUDDF-716G, Fujikin Incorporated, Japan) and the absolute pressure gauge as shown in Fig. 1a. The sheet, diaphragm, and body of the valve were made from Polychlorotrifluoroethylene (PCTFE), nickel-cobalt alloy, and stainless steel, respectively. The mother and daughter cylinders were connected and then the manifold was evacuated to  $\sim 10^{-4}$  Pa by a turbo molecular pump after all diaphragm valves opened (A1–A4 or a1–a6). The valve of the mother cylinder opened after the valves of A3 or a3 closed, and then the mixture was expanded from the mother cylinder to the daughter cylinder by opening the valve of the daughter cylinder. The transfer speed was controlled by degree of opening the diaphragm valve of the daughter cylinders and calculated roughly from the transfer time and volume. The valves of the mother and daughter cylinders closed immediately after the transfer volume reached the desired level which was confirmed by monitoring the weight of the daughter cylinder using a balance of load cell type (BW22KH, SHIMADZU Corporation, Japan) as shown in Fig. 1a. The transfer time and the pressure of the daughter cylinders were measured using a clock of PC and the absolute pressure gauge, respectively. The transfer volume was computed using the inner volume and the pressure of the daughter cylinder. Molar fractions of CO<sub>2</sub> in the mother cylinders were measured using the Picarro G2301 before starting each experiment, and after each experiment, those in the mother and daughter cylinders were measured several hours to half a day after the mixtures were transferred. The Picarro G2301 was calibrated using standard mixtures with atmospheric CO<sub>2</sub> levels before and after each transfer experiment. We also measured  $\delta(^{29}\text{N}_2/^{28}\text{N}_2)$ ,  $\delta(^{34}\text{O}_2/^{32}\text{O}_2)$ ,  $\delta(^{32}\text{O}_2/^{28}\text{N}_2)$ ,  $\delta(^{40}\text{Ar}/^{28}\text{N}_2)$ , and  $\delta(^{40}\text{Ar}/^{36}\text{Ar})$  in the mother and daughter cylinders using a mass spectrometer (Delta-V, Thermo Fisher Scientific Inc., USA) to clarify the mechanism(s) of diffusive fractionation during the mother–daughter experiment based on relationships between the measured elemental and isotopic ratios (e.g., Langenfelds et al., 2003; Ishidoya et al., 2013). The measurement details of the technique were provided in Ishidoya and Murayama (2014). The value of  $\delta(\text{CO}_2/\text{N}_2)$  was calculated using the ratio of CO<sub>2</sub>/N<sub>2</sub> obtained from Eq. (1) assuming that minor components except CO<sub>2</sub> can be ignored ( $\text{N}_2 + \text{O}_2 + \text{Ar} + \text{CO}_2 = 1$ ).

$$\text{CO}_2/\text{N}_2 = \frac{\text{CO}_2}{\text{N}_2} \times \frac{1-\text{CO}_2}{1-\text{CO}_2} = \frac{\text{CO}_2}{\text{N}_2} \times \frac{\text{N}_2 + \text{O}_2 + \text{Ar}}{1-\text{CO}_2} = \frac{\text{CO}_2}{1-\text{CO}_2} \times \left( 1 + \frac{\text{O}_2}{\text{N}_2} + \frac{\text{Ar}}{\text{N}_2} \right). \quad (1)$$

Where CO<sub>2</sub> molar fractions measured using Picarro G2301 were used as values of CO<sub>2</sub>. The ratios of O<sub>2</sub>/N<sub>2</sub> and Ar/N<sub>2</sub> were computed using values measured using the mass spectrometer (Aoki et al., 2019).

## 155 2.2 Preparation of standard mixtures

### 2.2.1 Starting Materials for preparation

Standard mixtures were gravimetrically prepared using the one-step and the three-step dilution in accordance with ISO 6142-1:2015. Pure CO<sub>2</sub> (>99.998 %, Nippon Ekitan Corp., Japan) and purified air (G1-grade, Japan Fine Products, Japan) were used as a source gas. The purity of pure CO<sub>2</sub> and N<sub>2</sub> molar fraction in the air was determined using a subtraction method in which the sum of molar fractions of impurities was subtracted from 1 (ISO 19229:2015). Impurities in the source gases were identified and quantified using gas chromatography (GC). A GC with a thermal conductivity detector (TCD) was used to analyze N<sub>2</sub>, O<sub>2</sub>, CH<sub>4</sub>, and H<sub>2</sub> in pure CO<sub>2</sub>. Ar in the air was analyzed using GC-TCD with an oxygen absorber. A paramagnetic oxygen analyzer was used to quantify O<sub>2</sub> in the air. A Fourier-transform infrared spectrometer was used to detect trace amounts of CO<sub>2</sub>, CH<sub>4</sub>, and CO in the air. A capacitance type moisture sensor was used to measure H<sub>2</sub>O in pure CO<sub>2</sub>, and a cavity ring-down moisture analyzer was used to measure H<sub>2</sub>O in the air.

### 2.2.2 Balances and weighing sequence

A 0.8-L aluminum cylinder and a 10-L aluminum cylinder were used for preparing standard mixtures with atmospheric CO<sub>2</sub> levels using a one-step dilution, while a 10-L cylinder was used for preparing a three-step dilution. The two types of cylinders were weighed using two different balances (mass comparators). One is AX2005 (Mettler Toledo, Switzerland) used for weighing the 0.8-L cylinder, of which resolution and maximum load are 0.01 mg and 2 kg, respectively. Another is the XP26003L (Mettler Toledo, Switzerland) used for weighing the 10-L cylinder, of which the resolution and maximum load are 1 mg and 26 kg (Matsumoto et al., 2004, Aoki et al., 2019), respectively. The mass measurement of each cylinder, which was performed in a weighing room controlled at temperature and humidity 26°C ± 0.5°C and 48 % ± 1 %, 175

respectively, was conducted with respect to a nearly identical reference cylinder to reduce any influence exerted by zero-point drifts, sensitivity issues associated with the mass comparator, changes in buoyancy acting on the cylinder, or adsorption effects on the cylinder's surface because of the presence of water vapor (Alink et al., 2000; Milton et al., 2011). This was performed based on several consecutive weighing operations in the ABBA order sequence, where "A" and "B" denote the reference and sample, respectively. The process of loading and unloading the cylinders was automated, and one complete cycle of the ABBA sequence took five minutes. The mass difference, which was calculated by subtracting the reference cylinder from the sample cylinder readings, provided the mass reading recorded from the weighing system. Aoki et al. (2019) reported that the mass reading deviates in relation to temperature differences between the sample and the surrounding air. In this study, the mass measurement was performed at the sample and the surrounding areas at the same temperature to reduce the deviation.

### 2.2.3 Preparation process by one-step dilution

Standard mixtures were gravimetrically prepared by mixing pure CO<sub>2</sub> and air using stainless steel manifolds (Fig 1b and Fig 1c) in the process shown in Fig. 2a. The pure CO<sub>2</sub> cylinder and the 0.8-L aluminum cylinder were connected at the position of valve 2 (V2) and valve 5 (V5) to the stainless-steel manifold (Fig. 1b) the internal surface of which was electropolished. The 0.8-L aluminum cylinder was evacuated to  $\sim 5.0 \times 10^{-5}$  Pa via the manifold by opening V2, V4, V5, and V6. The pure CO<sub>2</sub> was added to the 0.8-L aluminum cylinder after closing V4. Furthermore, we connected the 0.8-L cylinder and the evacuated 10-L cylinder at the position of V8, and then evacuated the manifold to  $\sim 5.0 \times 10^{-5}$  Pa by opening V4, V7, and V8. The movement of the 0.8-L cylinder was made to reduce the dead volume when the pure CO<sub>2</sub> was transferred to 10-L cylinder. The valves of the 0.8-L and 10-L cylinders were opened after closing V8, allowing the pure CO<sub>2</sub> to expand into the 10-L cylinder. Both cylinder valves were closed, and then the remaining CO<sub>2</sub> in the manifold was moved into the 10-L cylinder by alternating the pressurization–expansion operation that pressurizes the manifold to  $\sim 1.5$  MPa with air and open the valve of the 10-L cylinder. The 10-L cylinder was connected to other manifold shown in Fig. 1c after the CO<sub>2</sub> was completely transferred into



the cylinder by repeating this pressurization expansion process 300 times. The manifold was evacuated to  $\sim 1.5 \times 10^{-4}$  Pa and then the cylinder was further pressurized to  $\sim 10.0$  MPa with air using the manifold. The CO<sub>2</sub> mass filled into the 10-L cylinder was determined by weighing the 0.8-L cylinder before and after pure CO<sub>2</sub> was transferred, whereas the mass of air was calculated by subtracting the CO<sub>2</sub> mass from the difference in the 10-L cylinder mass before and after transferring pure CO<sub>2</sub> and air into the 10-L cylinder.

#### 2.2.4 Preparation process by three-step dilution

Fig. 2b shows that the standard mixtures were gravimetrically prepared into the 10-L cylinders by diluting pure CO<sub>2</sub> with air three times in the process by using the manifold shown in Fig. 1c. The preparation technique detail was provided in Matsumoto et al. (2004 and 2008) and Aoki et al. (2019). In the first step dilution, a gas mixture with a CO<sub>2</sub> molar fraction of  $65000 \mu\text{mol mol}^{-1}$ , referred to as a 1<sup>st</sup> gas mixture, was prepared from pure CO<sub>2</sub> and air. The pure CO<sub>2</sub> was transferred into the 10-L cylinder evacuated to  $1.5 \times 10^{-4}$  Pa, which was then pressurized to 10.0 MPa with air using the manifold shown in Fig. 1c. The masses of pure CO<sub>2</sub> and air were approximately 110 and 1100 g, respectively. In the second step, a gas mixture with a CO<sub>2</sub> molar fraction of  $5000 \mu\text{mol mol}^{-1}$ , referred to as a 2<sup>nd</sup> gas mixture, was prepared from the 1<sup>st</sup> gas mixture and air. The 1<sup>st</sup> gas mixture was transferred into the 10-L cylinder evacuated to  $1.5 \times 10^{-4}$  Pa, which was then pressurized to 10.0 MPa by air. The masses of the 1<sup>st</sup> gas mixture and air were approximately 100 and 1200 g, respectively. In the third step, a gas mixture with atmospheric CO<sub>2</sub> level, referred to as a 3<sup>rd</sup> gas mixture, was gravimetrically prepared from the 2<sup>nd</sup> gas mixture and air. The 2<sup>nd</sup> gas mixture was transferred into the 10-L cylinder evacuated to  $1.5 \times 10^{-4}$  Pa, which was then pressurized to 10.0 MPa with air. The masses of the 2<sup>nd</sup> gas mixture and air were approximately 100 and 1200 g, respectively. The mass of pure CO<sub>2</sub>, CO<sub>2</sub>/air mixture, and air used as source gases was determined by weighing the cylinder before and after filling each source gas.

### 2.2.5 Analysis of standard mixtures

225 The gravimetrically prepared standard mixtures (3<sup>rd</sup> gas mixtures) were measured using the Picarro G2301  
equipped with a multiport valve (Valco Instruments Co. Inc., USA) for gas introduction and a mass flow  
controller (SEC-N112, 100SCCM, Horiba STEC, CO., Ltd, Japan). The output of the Picarro G2301 was  
calibrated using standard mixtures prepared by the one-step dilution. CO<sub>2</sub> molar fractions in the 3<sup>rd</sup> gas  
mixtures were calculated from the calibration line obtained by applying the Deming least-square fit to the  
230 measured data. In the calibration, two series of standard mixtures were used. One series was composed of  
four standard mixtures with the range from 390  $\mu\text{mol mol}^{-1}$  to 430  $\mu\text{mol mol}^{-1}$  and another series was  
composed of five standard mixtures from 390  $\mu\text{mol mol}^{-1}$  to 420  $\mu\text{mol mol}^{-1}$ .

## 3 Result and discussion

### 3.1 Adsorption and fractionation of CO<sub>2</sub>/air mixtures

235 As described in the introduction, the adsorption of CO<sub>2</sub> on a cylinder's internal surface causes a small bias  
on the gravimetrically assigned CO<sub>2</sub> molar fraction. Furthermore, the transfer of CO<sub>2</sub>/air mixture changed  
CO<sub>2</sub> molar fractions by about 0.10  $\mu\text{mol mol}^{-1}$ . This allows transfer of source gases to have a larger impact  
on the CO<sub>2</sub> molar fractions than the bias on adsorption process. Therefore, we estimated the amount of CO<sub>2</sub>  
adsorbed on the internal surface of a 10-L aluminum cylinder, and then fully evaluated the amount of  
240 fractionation caused by the transfer of CO<sub>2</sub>/air mixtures used as source gases in the evacuated cylinders.

#### 3.1.1 Amount of CO<sub>2</sub> adsorbed on the internal surface of a cylinder

Previous studies have shown that by applying the Langmuir adsorption-desorption model to the results of  
decanting experiments, it is possible to determine the amount of CO<sub>2</sub> adsorbed on the internal surface of a  
cylinder. In this method, the amount of CO<sub>2</sub> adsorbed on the internal surfaces at the initial pressure of the  
245 decanting experiment is expressed as a molar fraction. For example, Schibig et al. (2018) performed a  
decanting experiment, emptying 29.5 L aluminum cylinders at a low flow rate of 300 mL min<sup>-1</sup> and high  
flow rate of 5 L min<sup>-1</sup>, which is estimated to be  $0.0165 \pm 0.0016 \mu\text{mol mol}^{-1}$  and  $0.043 \pm 0.008 \mu\text{mol mol}^{-1}$

at 15.0 MPa, respectively. Leuenberger et al. (2015) also performed the decanting experiment, emptying 30 L aluminum cylinders at a low flow rate of 250 mL min<sup>-1</sup> and high flow rate of 5 L min<sup>-1</sup>, which is estimated to be 0.028 μmol mol<sup>-1</sup> at 6.0 MPa and 0.047 μmol mol<sup>-1</sup> at 9.0 MPa, respectively. The low-flow decanting experiments indicated that less CO<sub>2</sub> was adsorbed on the internal surfaces of cylinders compared to the high-flow decanting experiments. They pointed out that the enrichment of CO<sub>2</sub> molar fraction detected in the high flow decanting experiment was related to thermal diffusion and fractionation in the cylinder. Previous studies showed that a low flow decanting experiment is suitable for evaluating the amount of CO<sub>2</sub> adsorbed on a cylinder internal surface in the case of 29.5 L and 30 L aluminum cylinders (Schibig et al., 2018; Leuenberger et al., 2015). It is not known whether this applies to the experiment using 10-L aluminum cylinders. Therefore, we investigated the optimum flow rate to evaluate the adsorbed amount by measuring CO<sub>2</sub> molar fraction in a gas mixture exiting from the 10-L cylinder at low flow rates of 80 mL min<sup>-1</sup>, 150 mL min<sup>-1</sup>, and 300 mL min<sup>-1</sup> during the decrease in pressure from 11.0 MPa to 0.1 MPa. The deviations in CO<sub>2</sub> molar fractions from initial values against relative cylinder pressure ( $P/P_0$ ) at different flow rates are shown in Fig. 3a. Where  $P$  is the actual pressure of the cylinder in MPa and  $P_0$  is the initial pressure of the cylinder in MPa before the decanting experiment. The CO<sub>2</sub> in the gas mixture flow increased by  $0.16 \pm 0.04$  μmol mol<sup>-1</sup> as the cylinder pressure decreased from 11.0 MPa to 0.1 MPa. Unless otherwise noted, the numbers following the symbol  $\pm$  represent standard deviation. The increase in CO<sub>2</sub> molar fraction is the same as flow rates of 80 mL min<sup>-1</sup>, 150 mL min<sup>-1</sup>, and 300 mL min<sup>-1</sup>, indicating that the contribution of thermal fractionation is negligible at a flow rate of 300 mL min<sup>-1</sup> or less. The amount adsorbed on the internal surface of the cylinder ( $X_{\text{CO}_2,\text{ad}}$ ) was calculated using the following equation based on the Langmuir model as derived by Leuenberger et al. (2015) (Fig. 3b).

$$X_{\text{CO}_2,\text{meas}} = X_{\text{CO}_2,\text{ad}} \cdot \left( \frac{K(P-P_0)}{1+K \cdot P} + (1 + K \cdot P_0) \cdot \ln \left( \frac{P_0 \cdot (1+K \cdot P)}{P \cdot (1+K \cdot P_0)} \right) \right) + X_{\text{CO}_2,\text{initial}} \quad (2)$$

Where  $X_{\text{CO}_2,\text{ad}}$  is expressed as the  $\text{CO}_2$  molar fraction multiplied by the occupied adsorption sites at pressure  $P_0$ .  $X_{\text{CO}_2,\text{meas}}$  corresponds to the measured molar fraction.  $X_{\text{CO}_2,\text{initial}}$  is the  $\text{CO}_2$  molar fraction measured in the cylinder at a pressure  $P_0$ .  $K$  is the ratio of the adsorption and desorption rate constants, and its unit is  $\text{MPa}^{-1}$ .  $X_{\text{CO}_2,\text{ad}}$  and  $K$  was obtained from the least square fit to the results. These experiments were performed seven times, and the average of  $X_{\text{CO}_2,\text{ad}}$  was  $0.027 \pm 0.004 \mu\text{mol mol}^{-1}$ , corresponding to 0.030 mL standard temperature and pressure (STP) or 1.2 micromoles or  $7.3 \times 10^{17}$  molecules. There was no difference among the values of  $X_{\text{CO}_2,\text{ad}}$  in range of  $\text{CO}_2$  from 350 to 450  $\mu\text{mol mol}^{-1}$ . The ratio of the adsorption of  $\text{CO}_2$  to total  $\text{CO}_2$  in the cylinder is  $0.008 \% \pm 0.001 \%$  at a unit of mole. The inner diameter of 0.16 m, length of 0.56 m, and the internal surface area are roughly calculated to be  $0.32 \text{ m}^2$ . The occupied area of  $\text{CO}_2$  adsorbed on the internal surface was estimated to be  $0.06 \text{ m}^2$ , assuming a molecule diameter of 0.34 nm, corresponding to approximately 20 % of the inner area by a monolayer of adsorbed  $\text{CO}_2$  molecules. The  $\text{CO}_2$  molar fractions in 3<sup>rd</sup> gas mixtures gravimetrically determined in the following section were computed considering the adsorbed amount by the third step dilution because the adsorption of  $\text{CO}_2$  causes a small bias of  $\text{CO}_2$  molar fraction in a cylinder. However, the amount was neglected in the case of the 1<sup>st</sup> and 2<sup>nd</sup> gas mixtures. This is because the  $\text{CO}_2$  molar fraction is significantly higher than the atmospheric  $\text{CO}_2$  level by 10 and 100 times or more. In the Langmuir model, the increase rate of the amount adsorbed on the internal surface with increasing the molar fraction of  $\text{CO}_2$  becomes small as that of  $\text{CO}_2$  is higher. The adsorbed amount is assumed to be lower than the adsorption ratio of  $0.008 \% \pm 0.001 \%$  in the case of the 1<sup>st</sup> and 2<sup>nd</sup> gas mixtures with a high molar fraction of  $\text{CO}_2$ .

### 3.1.2 Mother–daughter experiment.

The fractionation of  $\text{CO}_2$  and air is expected to result from the diffusive fractionation process based on the three types of diffusion, i.e., pressure diffusion, thermal diffusion, and effusion as described by Langenfelds et al. (2005) and Moore et al. (1962). The pressure diffusion is driven by a pressure gradient. The diffusion caused heavier molecules to be preferentially accumulated in the region of higher pressure. The thermal diffusion is driven by a temperature gradient. Heavier molecules are preferentially accumulated in the

colder region. The effusion is known as Knudsen diffusion. Gas molecules escaping from a pressurized vessel through a tiny orifice are subject to molecule effusion. However, the effusion was negligible in our mother–daughter experiments since this Knudsen diffusion occurs when the size of the orifice is small compared to the mean free path among molecular collisions. On the other hand, the temperature decreases of 2–8 K for the mother cylinders were observed during our mother–daughter experiments. This may allow the fractionation of CO<sub>2</sub> and air by the adsorption process. It is because the fractionation of the adsorption process is assumed to be caused by the increase in the amount of CO<sub>2</sub> adsorbed on the internal surface according to the cooling of the mother cylinder in the transfer of the gas mixture. Leuenberger et al. (2015) identified the temperature dependence in the amount of CO<sub>2</sub> adsorbed on the internal surface of an aluminum cylinder to be in a range from  $-0.0002 \mu\text{mol mol}^{-1} \text{K}^{-1}$  to  $-0.0003 \mu\text{mol mol}^{-1} \text{K}^{-1}$ . This corresponded to the decrease in  $0.0004 \mu\text{mol mol}^{-1}$ – $0.0024 \mu\text{mol mol}^{-1}$  for CO<sub>2</sub> molar fractions in the mixtures transferred from the mother cylinder, which is significantly lower than the changes in CO<sub>2</sub> molar fractions in the transfer of CO<sub>2</sub>/air mixtures detected by Hall et al. (2019).

Mother–daughter experiments of gas mixtures with atmospheric CO<sub>2</sub> levels were performed in fifteen sets using 48-L and 10-L aluminum cylinders as mother cylinders and 10-L aluminum cylinders as daughter cylinders: three sets were performed with horizontal placement of mother cylinders and twelve sets were with vertical placement. All transfers of the mixtures performed with horizontal placement increased the CO<sub>2</sub> molar fractions in the daughter cylinders from those before the transfer as shown in Fig. 4, while all transfer with vertical placement decreased the CO<sub>2</sub> molar fractions in the daughter cylinders. The CO<sub>2</sub> molar fractions deviated inversely in the transfers from the vertical mother cylinder and the horizontal mother cylinder. The difference in the deviations indicated that the fractionations occurred rather in the mother cylinders than in the transfer line and manifold since the pressure and thermal gradient in the mixtures in transfer line and manifold are determined regardless of the vertical and horizontal placement of mother cylinders. The direction of the pressure gradient does not change even if the placement of the mother cylinder changes the magnitude of the pressure gradient in the mother cylinder. The fact that the deviation of CO<sub>2</sub> molar fraction was opposite suggests that the fractionation of CO<sub>2</sub> and air was caused based on

rather the thermal diffusion than the pressure diffusion. A source gas used for preparation of standard mixtures are generally transfers into a vertical receiving cylinder from a vertical mother cylinder. The experiments for the mother cylinders with vertical placement were conducted at different mother cylinder's pressure, transfer gas amount, and transfer gas speed corresponding to transfer conditions of a source gas, to understand the contributions of the fractionation to CO<sub>2</sub> molar fraction in general preparation process. The mother–daughter experimental results performed with vertical placement are summarized in Table 1. Here, CO<sub>2</sub> molar fractions in the daughter cylinders were corrected by the amount of CO<sub>2</sub> absorbed on the internal surface based on the value of  $0.027 \pm 0.004 \mu\text{mol mol}^{-1}$  determined by the decanting experiment. The dependence of CO<sub>2</sub> molar fractions in the daughter cylinders relative to transfer volume, cylinder pressure, and transfer speed is shown in Fig. 4. The closed circles in Fig. 4 represent values in the transfer speed of more than  $19 \text{ L min}^{-1}$ , whereas open triangles represent values in the transfer speed of less than  $3 \text{ L min}^{-1}$ . All CO<sub>2</sub> molar fractions in the mixtures transferred into the daughter cylinders decreased from the CO<sub>2</sub> molar fraction before the transfer of the mixtures as shown in Fig. 4. The decrease in CO<sub>2</sub> molar fractions mixtures for the daughter cylinders was  $0.122 \pm 0.040 \mu\text{mol mol}^{-1}$  on average at a transfer speed of more than  $19 \text{ L min}^{-1}$ , whereas the decrease in CO<sub>2</sub> molar fractions for daughter cylinders from initial values became significantly small as  $0.036 \pm 0.027 \mu\text{mol mol}^{-1}$  ( $0.008 \% \pm 0.006 \%$ ) on average when the mixtures were transferred at an extremely slow transfer speed of less than  $3 \text{ L min}^{-1}$ . The decreased values at the transfer speed of more than  $19 \text{ L min}^{-1}$  agreed with previous values of  $0.10$  and  $0.13 \mu\text{mol mol}^{-1}$  reported by Hall et al. (2019), who reported that the decrease could be related to thermal diffusion. Correspondingly, the remaining mixtures in all vertical mother cylinders provided higher CO<sub>2</sub> molar fractions than before the transfer of the mixture, contrary to the daughter cylinders. The amount of substance ( $n$ ) for increased and decreased CO<sub>2</sub> in the mother and daughter cylinders was computed from the change amount of CO<sub>2</sub> molar fraction ( $c_{\text{CO}_2}$ ) to evaluate the mass balance of CO<sub>2</sub> corresponding to increase and decrease in CO<sub>2</sub> molar fractions, which is related to the initial value before the transfer of the mixture, and the cylinder volume ( $V$ ) and pressure ( $p$ ) in the daughter cylinder using the ideal gas law;  $n = c_{\text{CO}_2} \times p \times V / (R \times T)$ . Where  $R$  and  $T$  express gas constant ( $0.082057 \text{ L atm K}^{-1} \text{ mol}^{-1}$ ) and gas

temperature (298 K), respectively. The mass balance between the increase and decrease was consistent  
350 within uncertainties in each experiment (Table 1), indicating that the changes of CO<sub>2</sub> were caused by the  
diffusive fractionation rather than CO<sub>2</sub> adsorption.

As shown in Fig. 4, the CO<sub>2</sub> decrease does not depend on the transfer volume and initial pressure of the  
mother cylinder, but it becomes significantly smaller below flow rates of 19 L min<sup>-1</sup>. The fact that the  
amount of CO<sub>2</sub> molar fractions decreased was constant regardless of the transfer volume, indicates that the  
355 fractionation factor did not change at the beginning and end of the transfer. The change of CO<sub>2</sub> decreased  
amounts due to transfer speed also support that the fractionation is caused by thermal diffusion because the  
transfer speed determines the thermal gradient. Source gases transfer into daughter cylinders at the transfer  
speed of more than 19 L min<sup>-1</sup> in general preparation process. Therefore, CO<sub>2</sub> molar fractions in standard  
mixtures with accurate atmospheric CO<sub>2</sub> level are influenced by the fractionation in transfer of the source  
360 gas but it may be significantly suppressed by the transfer of the mixture at a lower transfer speed. However,  
it is difficult to transfer source gases at the transfer speed presented in this experiment because the speed is  
much lower than the normal transfer speed in the preparation process of the standard mixtures. We must  
acquire a technique to control the transfer speed of source gas.

A fractionation factor ( $\alpha$ ) in the transfer of a source gas was estimated from the results for the transfer speed  
365 of more than 19 L min<sup>-1</sup> because a source gas in the actual preparation of standard mixtures is transferred  
at the transfer speed larger than 19 L min<sup>-1</sup>. CO<sub>2</sub> molar fraction in the gas mixture in the cylinder ( $X_{out}$ ) is  
modified by the fractionation factor to the ratio in the cylinder as the following equation.

$$X_{out} = \alpha X_0. \quad (3)$$

370

Where  $X_0$  is the initial CO<sub>2</sub> molar fractions. The fractionation factor ( $\alpha$ ) was estimated to be  $X_{out}/X_0 = 0.99968 \pm 0.00010$  using only values with transfer speeds of more than 19 L min mol<sup>-1</sup> in Table 1. If a  
standard mixture with a CO<sub>2</sub> molar fraction of 400  $\mu\text{mol mol}^{-1}$  is prepared by a three-step dilution, the CO<sub>2</sub>  
molar fraction in the standard mixture is predicted to decrease by  $0.252 \pm 0.082 \mu\text{mol mol}^{-1}$  by the

375 fractionation effect in the second and third step dilutions. Additionally, the CO<sub>2</sub> molar fraction in a source  
gas ( $X$ ) can be expressed using pressure ( $P$ ) and initial pressure ( $P_0$ ) of the source gas by the Rayleigh  
fractionation model.

$$\frac{X}{X_0} = \left(\frac{P}{P_0}\right)^{\alpha-1} \quad (4)$$

380

According to equation (4), the CO<sub>2</sub> molar fraction in the source gas is estimated to be  $1.00076 \pm 0.00024$   
against an initial value with a decrease in pressure from 11.0 to 1.0 MPa. This value corresponds to the  
increase in  $0.30 \pm 0.09 \mu\text{mol mol}^{-1}$  from the initial value in a standard mixture with a CO<sub>2</sub> molar fraction  
of  $400 \mu\text{mol mol}^{-1}$  prepared from the source gas.

385 We also measured different molecular pairs,  $^{32}\text{O}_2/^{28}\text{N}_2$ ,  $^{40}\text{Ar}/^{28}\text{N}_2$ , and  $\text{CO}_2/\text{N}_2$ , and the same molecular pairs,  
 $^{29}\text{N}_2/^{28}\text{N}_2$ ,  $^{34}\text{O}_2/^{32}\text{O}_2$ , and  $^{40}\text{Ar}/^{36}\text{Ar}$  to confirm if the fractionating process discussed above occurred by the  
transfer of mixture. The relationship of the deviations of  $\delta(^{32}\text{O}_2/^{28}\text{N}_2)$ ,  $\delta(^{40}\text{Ar}/^{28}\text{N}_2)$ ,  $\delta(\text{CO}_2/\text{N}_2)$ ,  $\delta(^{34}\text{O}_2/^{32}\text{O}_2)$ ,  
and  $\delta(^{40}\text{Ar}/^{36}\text{Ar})$  with deviations of  $\delta(^{29}\text{N}_2/^{28}\text{N}_2)$  in the daughter cylinders relative to their mother cylinders  
are shown in Fig. 5. The black line represents the values obtained from the mother–daughter experiment  
390 using 10 and 48 L cylinders. The red dotted line represents the theoretical value of thermal diffusion, which  
was calculated using the equations provided by Langenfelds et al. (2005). Red solid lines represent the  
deviations due to thermal diffusion experimentally estimated by Ishidoya et al. (2013, 2014). The deviation  
of molecular pairs in the daughter cylinders relative to their mother cylinders occurred between not only  
different molecular pairs,  $\delta(^{32}\text{O}_2/^{28}\text{N}_2)$ ,  $\delta(^{40}\text{Ar}/^{28}\text{N}_2)$ , and  $\delta(\text{CO}_2/\text{N}_2)$  but also the same molecular pairs,  
395  $\delta(^{29}\text{N}_2/^{28}\text{N}_2)$ ,  $\delta(^{34}\text{O}_2/^{32}\text{O}_2)$ , and  $\delta(^{40}\text{Ar}/^{36}\text{Ar})$ , suggesting that the deviation corresponded to the mass number  
of the molecules. The relationship of the deviations closed to the experimental thermal diffusion, supporting  
that the fractionation occurs due to thermal diffusion. The deviations of  $\delta(\text{CO}_2/\text{N}_2)$  were more than the  
values expected from theoretical and experimental thermal diffusions. It may be because the deviation of the  
experimental thermal diffusion for  $\delta(\text{CO}_2/\text{N}_2)$  had larger uncertainty than those of other species. The values



400 of  $\delta(^{32}\text{O}_2/^{28}\text{N}_2)$  and  $\delta(^{40}\text{Ar}/^{28}\text{N}_2)$  scattered more than their uncertainties. Further studies are needed to  
understand the mechanism(s) of the fractionation in detail.

### 3.2 Comparison between one-step dilution and three-step dilutions

In the previous section, we determined the fractionation factor in the transfer of a source gas to be  $0.99968 \pm 0.00010$ . This indicates that the  $\text{CO}_2$  molar fraction in gravimetrically prepared standard mixture with  
405 atmospheric  $\text{CO}_2$  level has a systematic error by the fractionation in the dilution process by the transfer of  
 $\text{CO}_2$ /air mixture used as a source gas to an evacuated daughter cylinder in the second and third step dilution.  
Two types of experiments were conducted to confirm the systematic error. One evaluated the fractionation  
in the second and third step dilutions based on the increase in  $\text{CO}_2$  molar fractions in 1<sup>st</sup> and 2<sup>nd</sup> gas mixtures  
due to the fractionation with their consumption. Another demonstrated that  $\text{CO}_2$  molar fractions in 3<sup>rd</sup> gas  
410 mixtures deviate from their gravimetric values by measuring 3<sup>rd</sup> gas mixtures based on standard mixtures  
prepared by one-step dilution, which can avoid the fractionation.

Two series of standard mixtures were prepared by one-step dilution to determine  $\text{CO}_2$  molar fractions in  
the 3<sup>rd</sup> gas mixtures used in the two experiments. The  $\text{CO}_2$  molar fractions were corrected on the basis of  
the adsorption of  $\text{CO}_2$  to the internal surface using the  $X_{\text{CO}_2,\text{ad}}$  of  $0.027 \pm 0.004 \mu\text{mol mol}^{-1}$ . Four standard  
415 mixtures were prepared as the first series to evaluate the fractionation in the second and third steps, and the  
 $\text{CO}_2$  molar fractions were  $390.687 \pm 0.077 \mu\text{mol mol}^{-1}$ ,  $402.253 \pm 0.078 \mu\text{mol mol}^{-1}$ ,  $415.452 \pm 0.080 \mu\text{mol mol}^{-1}$ , and  
 $426.602 \pm 0.082 \mu\text{mol mol}^{-1}$ . Five standard mixtures were prepared as the second series to  
demonstrate the deviations of  $\text{CO}_2$  molar fractions in the 3<sup>rd</sup> gas mixtures in which the  $\text{CO}_2$  molar fractions  
were  $390.599 \pm 0.078 \mu\text{mol mol}^{-1}$ ,  $399.807 \pm 0.094 \mu\text{mol mol}^{-1}$ ,  $402.724 \pm 0.094 \mu\text{mol mol}^{-1}$ ,  $406.021 \pm$   
420  $0.094 \mu\text{mol mol}^{-1}$ , and  $419.618 \pm 0.098 \mu\text{mol mol}^{-1}$ . The numbers following the symbol  $\pm$  denote expanded  
uncertainty, which was mainly associated with the mass of source gases,  $\text{CO}_2$  and air. The molar mass of  
air also contributes to the uncertainty of the  $\text{CO}_2$  molar fraction because the composition of the air is  
different among individual cylinders purchased from the same gas manufacturer. For example,  $\text{O}_2$  molar  
fractions in the air which our laboratory uses, ranges from  $208000 \mu\text{mol mol}^{-1}$  to  $209600 \mu\text{mol mol}^{-1}$ . This

425 difference causes the CO<sub>2</sub> molar fraction to deviate by 0.09 μmol mol<sup>-1</sup>. Therefore, the molar fractions of  
N<sub>2</sub>, O<sub>2</sub>, and Ar in the air used in this experiment were determined based on standard mixtures composed of  
N<sub>2</sub>, O<sub>2</sub>, Ar, and CO<sub>2</sub>. Ar molar fractions were determined to range from 9300 μmol mol<sup>-1</sup> to 9360 μmol  
mol<sup>-1</sup> using GC-TCD, and their largest standard uncertainty was 6 μmol mol<sup>-1</sup>, whereas O<sub>2</sub> molar fractions  
430 analyzer and their largest standard uncertainty was 6 μmol mol<sup>-1</sup>. N<sub>2</sub> molar fractions in the air were  
calculated by subtracting the Ar and O<sub>2</sub> molar fractions from 1. The first and second series were measured  
using the Picarro G2301, showing the results in Fig. 6a. The line represents the Deming least-square fit to  
the data. The residuals from the line are shown in Fig. 6b. The error bar is expressed as the expanded  
uncertainty of gravimetric values. The residual ranges from -0.014 μmol mol<sup>-1</sup> to 0.008 μmol mol<sup>-1</sup> for the  
435 first series and from -0.057 μmol mol<sup>-1</sup> to 0.054 μmol mol<sup>-1</sup> for the second series. The measured molar  
fractions were consistent with the line within the expanded uncertainties.

To evaluate the increase in CO<sub>2</sub> molar fraction in 2<sup>nd</sup> gas mixture as the source gas, six reference mixtures  
(3<sup>rd</sup> gas mixtures) with approximately 400 μmol mol<sup>-1</sup> were prepared from a common 2<sup>nd</sup> gas mixture,  
which had a gravimetric value of 5022.46 ± 0.18 μmol mol<sup>-1</sup> for CO<sub>2</sub> in the process shown in Fig. 7a. The  
440 number following the symbol ± denotes the expanded uncertainty. The pressure of the 2<sup>nd</sup> gas mixture used  
for the preparation of the 3<sup>rd</sup> gas mixtures was 11.5 MPa, 9.7 MPa, 8.05 MPa, 4.2 MPa, 2.75 MPa, and 1.1  
MPa. The increase in CO<sub>2</sub> molar fractions in the 2<sup>nd</sup> gas mixture was evaluated by measuring the 3<sup>rd</sup> gas  
mixtures using the Picarro G2301 based on the first series because the increase in the 2<sup>nd</sup> gas mixture  
directly reflects them in the 3<sup>rd</sup> gas mixtures prepared from the 2<sup>nd</sup> gas mixture. The fractionation in the  
445 transfer of the 2<sup>nd</sup> gas mixture into the daughter cylinder contributes to not the increase of CO<sub>2</sub> molar  
fraction in the 3<sup>rd</sup> gas mixture but that of CO<sub>2</sub> molar fraction in the remaining 2<sup>nd</sup> gas mixture because the  
effects on the transferred mixtures act similarly on all 3<sup>rd</sup> gas mixtures. The relationship of the deviations  
from the gravimetric values in the 3<sup>rd</sup> gas mixtures and the pressure of the 2<sup>nd</sup> gas mixture is shown in Fig.  
8a. The vertical axis is expressed as the deviation values to subtract the measured values from the  
450 gravimetric values for the 3<sup>rd</sup> standard mixtures. The error bars represent the expanded uncertainties

calculated based on combining the standard uncertainty of the measurement with that of the gravimetric values for the standard mixtures prepared by a three-step dilution. The known negative offset from the gravimetric value caused by the fractionation process in the gas transfer during the 3<sup>rd</sup> gas mixture preparation is observed for the 3<sup>rd</sup> gas mixture prepared from the 2<sup>nd</sup> at 11.5 MPa. With decreasing the pressure of 2<sup>nd</sup> gas mixture to 1.1 MPa, CO<sub>2</sub> increased in the 3<sup>rd</sup> gas mixture by  $0.25 \pm 0.10 \mu\text{mol mol}^{-1}$ , which agrees with the increased value of  $0.30 \pm 0.10 \mu\text{mol mol}^{-1}$  predicted from Eq. (4) using the fractionation factor of  $0.99968 \pm 0.00010$  determined in section 3.1. However, we estimated the fractionation factor in the third step dilution by applying the Rayleigh fractionation model [the Eq. (4)] to the increase of the CO<sub>2</sub> mole fraction with the decrease of inner pressure, as shown in the solid line in Fig. 8a. The estimated fractionation factor was  $0.99975 \pm 0.00004$ , which was consistent with the fractionation factor of  $0.99968 \pm 0.00010$  estimated in section 3.1. This consistency indicates that the fractionation detected in the mother–daughter experiment also occurs in the transfer of a source gas in the preparation process of the 3<sup>rd</sup> gas mixtures.

The fractionation of CO<sub>2</sub> and air is also assumed to occur in the second step dilution in which the 1<sup>st</sup> gas mixture composed of CO<sub>2</sub> and air was transferred to the evacuated cylinder. We evaluated the fractionation based on the change in the deviations from the gravimetric values in 3<sup>rd</sup> gas mixtures prepared using the process shown in Fig. 7b. Two 3<sup>rd</sup> gas mixtures with a CO<sub>2</sub> molar fraction of approximately  $400 \mu\text{mol mol}^{-1}$  were prepared from two 2<sup>nd</sup> gas mixtures, which were prepared using a common 1<sup>st</sup> gas mixture having a CO<sub>2</sub> molar fraction of  $65164.9 \pm 1.9 \mu\text{mol mol}^{-1}$ . The 2<sup>nd</sup> gas mixtures had CO<sub>2</sub> molar fractions of  $5022.46 \pm 0.18 \mu\text{mol mol}^{-1}$  and  $4824.67 \pm 0.35 \mu\text{mol mol}^{-1}$ , which were prepared from the 1<sup>st</sup> gas mixture at a pressure of 7.8 and 0.8 MPa. The 2<sup>nd</sup> gas mixtures were used only for the preparation of the 3<sup>rd</sup> gas mixtures. The number following the symbol  $\pm$  denotes the expanded uncertainty. The CO<sub>2</sub> molar fractions in the 3<sup>rd</sup> gas mixtures were determined using the Picarro G2301, which is based on the first series. The contribution of the fractionation of CO<sub>2</sub> in the daughter cylinder was canceled because of the reasons described in the previous paragraph. The relationship of the deviations in the measured values from the corresponding gravimetric values and pressure of the 1<sup>st</sup> gas mixture is shown in Fig. 8b. The solid and dotted lines in Fig.

8b represent the Rayleigh model line, which was calculated based on the fractionation factor of  $0.99975 \pm 0.00004$  and  $0.99968 \pm 0.00010$ . The error bars represent the expanded uncertainties calculated based on the combination of standard uncertainty of the measurement with that of the gravimetric values for the 3<sup>rd</sup> gas mixtures. The deviations increased by  $0.16 \pm 0.10 \mu\text{mol mol}^{-1}$  as the pressure decreased from 7.8 MPa to 0.8 MPa. Both lines agree with the deviations within the uncertainties. The results mean that the fractionation factor in the second step dilution is equivalent to the fractionation factor in the third step dilution. This means that fractionation occurs regardless of the CO<sub>2</sub> molar fraction of a source gas.

Finally, we demonstrated that the CO<sub>2</sub> molar fraction in the 3<sup>rd</sup> gas mixture deviated from its gravimetric value according to the fractionation factors described above. In this demonstration, four 3<sup>rd</sup> gas mixtures for atmospheric CO<sub>2</sub> levels were newly prepared by three-step dilutions. The increase in CO<sub>2</sub> molar fractions in the 1<sup>st</sup> and 2<sup>nd</sup> gas mixtures with their consumption were corrected on the basis of the decrease in their pressures from the initial values. The decreases in CO<sub>2</sub> molar fractions by the adsorption of CO<sub>2</sub> to the internal surface for 3<sup>rd</sup> gas mixtures were corrected based on the  $X_{\text{CO}_2,\text{ad}}$  of  $0.027 \pm 0.004 \mu\text{mol mol}^{-1}$ . These corrections allow for extracting only the deviations from gravimetric values caused by fractionation in the transfer of 1<sup>st</sup> and 2<sup>nd</sup> gas mixtures. The CO<sub>2</sub> molar fractions in the 3<sup>rd</sup> gas mixtures were measured using the Picarro G2301 based on the second series. The measured values of CO<sub>2</sub> molar fractions were calculated based on the calibration line obtained by applying the Deming least-square fit to the measured values. The error bars represent the expanded uncertainties of the gravimetric values. The deviations were  $-0.207 \pm 0.060 \mu\text{mol mol}^{-1}$  on average. The deviation was dropped between  $-0.252 \pm 0.082 \mu\text{mol mol}^{-1}$  and  $-0.200 \pm 0.032 \mu\text{mol mol}^{-1}$  calculated using the fractionation factor of  $0.99968 \pm 0.00010$  and  $0.99975 \pm 0.00004$ , and it was consistent with both values within their uncertainty. This indicates that the fractionation of CO<sub>2</sub> and air occurs according to our estimated fractionation factor in each dilution process.

#### 4 Conclusion

CO<sub>2</sub> adsorption on cylinder and fractionation of CO<sub>2</sub> and air were used to evaluate systematic deviations during the preparation of a standard mixture with atmospheric CO<sub>2</sub> levels. Decanting experiments were

performed to evaluate the amount of CO<sub>2</sub> adsorbed on the internal surface of a 10-L aluminum cylinder during the preparation of CO<sub>2</sub>/air mixtures at the atmospheric level. The amount of adsorbed CO<sub>2</sub> was determined to be  $0.027 \pm 0.004 \mu\text{mol mol}^{-1}$  at 11.0 MPa, resulting in a small bias in the gravimetric value.

505 The mother–daughter experiments were performed to understand the fractionation of CO<sub>2</sub> and air when a CO<sub>2</sub>/air mixture used was transferred into an evacuated cylinder as a source gas. CO<sub>2</sub> molar fractions in the mother and daughter cylinders increased and decreased, respectively, indicating that fractionation causes not only a decrease in CO<sub>2</sub> molar fraction in the prepared standard mixture but also an increase in CO<sub>2</sub> molar fraction in a remaining source gas. The decreases of CO<sub>2</sub> mole fractions in the daughter cylinders

510 were constant regardless of the transfer volume, the initial pressure of the mother cylinder, and the transfer speeds at flow rate exceeding  $19 \text{ L min}^{-1}$  which are in range of conditions used in preparation of the standard mixtures. This indicates that the degree of fractionation in transfer of a source gas is constant. We demonstrated that CO<sub>2</sub> molar fractions in standard mixtures by three-step dilutions decreased by  $-0.207 \pm 0.060 \mu\text{mol mol}^{-1}$  from gravimetric values based on source gas fractionation, which is greater than the

515 compatibility goal of  $0.1 \mu\text{mol mol}^{-1}$ . The decrease was between the values calculated using two fractionation factors of  $0.99976 \pm 0.00004$  and  $0.99968 \pm 0.00010$ ; one was estimated in mother–daughter transfer experiment and another was computed by applying the Rayleigh model to the increase in CO<sub>2</sub> molar fractions in source gas. Fractionation at different stages of a multi-step dilution can result in CO<sub>2</sub> increases as well as in CO<sub>2</sub> decreases of the final gas mixture. This affects the reproducibility and accuracy of CO<sub>2</sub>

520 molar fractions in gravimetric standard gases. CO<sub>2</sub> molar fractions in standard mixtures prepared by multistep dilutions were identified as including systematic error according to the fractionation of CO<sub>2</sub> and air. Therefore, we must consider the fractionation when determining CO<sub>2</sub> molar fraction in standard mixtures gravimetrically prepared by multistep dilutions.

## Code availability

525 **Data availability.** The data presented in this article are available upon request to Nobuyuki Aoki (aoki-nobu@aist.go.jp).

**Author contribution.** NA designed the study. NA performed the experiment and drafted the paper. SI carried out measurement by a mass spectrometry. NM helped with the preparation of standard mixtures. SM helped with determination of CO<sub>2</sub> molar fraction. All were actively involved with the final version of  
530 the paper.

**Competing interests.** The authors declare that they have no conflict of interest.

## Disclaimer

## Acknowledgments

This study was partly supported by the Global Environment Research Account for National Institutes of  
535 the Ministry of the Environment, Japan (grant nos. METI1454 and METI1953) and the JSPS KAKENHI Grant Number 19K05554.

## References

Aoki, N., and Shimosaka, T.: Development of an analytical system based on a paramagnetic oxygen analyzer for atmospheric oxygen variations, *Anal. Sci.*, 34, 487–493,  
540 <https://doi.org/10.2116/analsci.17P380>, 2018.

Aoki, N., Ishidoya, S., Matsumoto, N., Watanabe, T., Shimosaka, T., and Murayama, S.: Preparation of primary standard mixtures for atmospheric oxygen measurements with less than 1  $\mu\text{mol mol}^{-1}$  uncertainty for oxygen molar fractions, *Atmos. Meas. Tech.*, 12, 2631–2626, <https://doi.org/10.5194/amt-12-2631-2019>, 2019.

545 Alink, A., and Van der Veen, A. M.: Uncertainty calculations for the preparation of primary gas mixtures, *Metrologia*, 37, 641–650, <https://doi.org/10.1088/0026-1394/37/6/1>, 2000.

- Brewer, P. J., Brown, R. J. C., Resner, K. V., Hill-Pearce, R. E., Worton, D. R., Allen, N. D. C., Blakley, K. C., Benucci, D., and Ellison, M. R.: Influence of pressure on the composition of gaseous reference materials, *Anal. Chem.*, 90, 3490–3495, <https://doi.org/10.1021/acs.analchem.7b05309>, 2018.
- 550 Flores, E., Viallon, J., Choteau, T., Moussay, P., Idrees, F., Wielgosz, R., Lee, J., Zalewska, E., Nieuwenkamp, G., van der Veen, A., Konopelko, L. A., Kustikov, Y. A., Kolobova, A. V., Chubchenko, Y. K., Efremova, O. V., Zhe, B., Zhou, Z., Miller Jr, W. R., Rhoderick, G. C., Hodge, J. T., Shimosaka, T., Aoki, N., Hall, B., Brewer, P., Cieciora, D., Segal, M., Macé, T., Fükő, J., Szilágyi, Z. N., Büki, T., Jozela, M. I., Ntsasa, N. G., Leshabane, N., Tshilongo, J., Johri, P., and Tarhan, T.: CCQM-K120 (carbon dioxide
- 555 at background and urban level), *Metrologia*, 56, Number 1A, 2019.
- Hall, B. D., Crotwell, A. M., Miller, B. R., Schibig, M., and Elkins, J.: Gravimetrically prepared carbon dioxide standards in support of atmospheric research, *Atmos. Meas. Tech.*, 12, 517–524, <https://doi.org/10.5194/amt-12-517-2019>, 2019.
- Ishidoya, S., Sugawara, S., Morimoto, S., Aoki, S., Nakazawa, T., Honda, H., Sawa, Y., Niwa, Y., Saito,
- 560 K., Tsuji, K., Nishi, H., Baba, Y., Takatsuji, S., Dehara, K., and Fujiwara, H.: Gravitational separation in the stratosphere – A new indicator of atmospheric circulation, *Atmos. Chem. Phys.*, 13, 8787–8796, 2013.
- Ishidoya, S., and Murayama, S.: Development of a new high precision continuous measuring system for atmospheric O<sub>2</sub>/N<sub>2</sub> and Ar/N<sub>2</sub> and its application to the observation in Tsukuba, Japan, *Tellus B: Chem. Phys. Meteorol.*, 66, 22574, <https://doi.org/10.3402/tellusb.v66.22574>, 2014.
- 565 Ishidoya, S., Tsuboi, K., Matsueda, H., Murayama, S., Aoki, S., Nakazawa, T., Honda, H., Sawa, Y., Niwa, Y., Saito, K., Tsuji, K., Nishi, H., Baba, Y., Takatsuji, S., Dehara, K., and Fujiwara, H.: New atmospheric O<sub>2</sub>/N<sub>2</sub> ratio measurements over the western North Pacific using a cargo aircraft C-130H. *SOLA*. 10, 23–28, [doi:10.2151/sola.2014-006](https://doi.org/10.2151/sola.2014-006), 2014.
- ISO 6142-1:2015, Gas Analysis – Preparation of calibration gas mixtures – Part 1: gravimetric method for
- 570 class I mixtures, International Organization for Standardization, ISO 6142–1:2015.
- ISO 19229:2015, Gas analysis – Purity analysis and the treatment of purity data, International Organization for Standardization, ISO 19229:2015.

- Keeling, R. F., Blaine, T., Paplawsky, B., Katz, L., Atwood, C., and Brockwell, T.: Measurement of changes in atmospheric Ar/N<sub>2</sub> ratio using a rapid-switching, single-capillary mass spectrometer system, *Tellus* 56 B, 322–338, <https://doi.org/10.3402/tellusb.v56i4.16453>, 2004
- 575 B, 322–338, <https://doi.org/10.3402/tellusb.v56i4.16453>, 2004
- Keeling, R. F., Manning, A. C., Paplawsky, W. J., and Cox, A.: On the long-term stability of reference gases for atmospheric O<sub>2</sub>/N<sub>2</sub> and CO<sub>2</sub> measurements, *Tellus*. 59 B, 3–14, <https://doi.org/10.1111/j.1600-0889.2006.00196.x>, 2007.
- Langenfelds, R. L., van der Schoot, M. V., Francey, R. J., Steele, L. P., Schmidt, M., and Mukai, H.: Modification of air standard composition by diffusive and surface processes, *J. Geophys. Res. Atmos.*, 110, D13307, <https://doi.org/10.1029/2004JD005482>, 2005.
- 580 D13307, <https://doi.org/10.1029/2004JD005482>, 2005.
- Langmuir, I.: The adsorption of gases on plane surfaces of glass, mica and platinum, *J. Am. Chem. Soc.*, 40, 1361–1403, <https://doi.org/10.1021/ja02242a004>, 1918.
- Leuenberger, M. C., Schibig, M. F., and Nyfeler, P.: Gas adsorption and desorption effects on cylinders and their importance for long-term gas records, *Atmos. Meas. Tch.*, 8, 5289–5299, <https://doi.org/10.5194/amt-8-5289-2015>, 2015.
- 585 and their importance for long-term gas records, *Atmos. Meas. Tch.*, 8, 5289–5299, <https://doi.org/10.5194/amt-8-5289-2015>, 2015.
- Matsumoto, N., Watanabe, T., Maruyama, M., Horimoto, Y., Maeda, T., and Kato, K.: Development of mass measurement equipment using an electronic mass-comparator for gravimetric preparation of standard mixtures, *Metrologia*, 41, 178–188, <https://doi.org/10.1088/0026-1394/41/3/011>, 2004.
- 590 Matsumoto, N., Shimosaka, T., Watanabe, T., and Kato, K.: Evaluation of error sources in a gravimetric technique for preparation of a standard mixture (carbon dioxide in synthetic air), *Anal. Bioanal Chem.*, 391, 2061–2069, doi: 10.1007/s00216-008-2107-8, <https://doi.org/10.1007/s00216-008-2107-8>, 2008.
- Milton, M. J. T., Vargha, G. M., and Brown, A. S.: Gravimetric methods for the preparation of standard gas mixtures, *Metrologia*, 48, R1–R9, <https://doi.org/10.1088/0026-1394/48/5/R01>, 2011.
- 595 Miller, W. R., Rhoderick, G. C., and Guenther, F. R.: Investigating adsorption/desorption of carbon dioxide in aluminum compressed gas cylinders, *Anal. Chem.*, 87, 1957–1962, <https://doi.org/10.1021/ac504351b>, 2015.

Moore, W. J. (1962), *Physical Chemistry*, 4<sup>th</sup> ed., Pitman, London.



Schibig, M. F., Kitzis, D., and Tans, P. P.: Experiments with CO<sub>2</sub>-in-air reference gases in high-pressure aluminum cylinders, *Atmos. Meas. Tech.*, 11, 5565–5586, <https://doi.org/10.5194/amt-11-5565-2018>, 2018.

Tohjima, Y., Machida, T., Mukai, H., Maruyama, M., Nishino, T., Akama, I., Amari, T., and Watai, T.: Preparation of Gravimetric CO<sub>2</sub> Standards by One-Step Dilution Method, In: John B. Miller eds. 13th IAEA/WMO Meeting of CO<sub>2</sub> Experts, Vol WMO-GAW Report 168. Boulder, 2005, 26–32, 2006.

Tsuboi, K., Nakazawa, T., Matsueda, H., Machida, T., Aoki, S., Morimoto, S., Goto, D., Shimosaka, T., Kato, K., Aoki, N., Watanabe, T., Mukai, H., Tohjima, Y., Katsumata, K., Murayama, S., Ishidoya, S., Fujitani, T., Koide, H., Takahashi, M., Kawasaki, T., Takizawa, A., and Sawa, Y.: Inter comparison experiments for greenhouse gases observation (iceGGO) in 2012–2016, Technical Reports of the Meteorological Research Institute, 79, 2017, doi:10.11483/mritechrepo.79

WMO: 20th WMO/IAEA Meeting on Carbon Dioxide, Other Greenhouse Gases and Related Tracers Measurement Techniques (GGMT-2019), GAW Report, No. 255, 2020.

Table 1. Results of the mother–daughter experiment on 10-L and 48-L aluminum cylinders which were performed the mother cylinder with vertical placement. CO<sub>2</sub>/air mixtures at atmospheric level were transferred from 10-L or 48-L aluminum cylinders (mother) to 10-L aluminum cylinders (daughter) at different mother cylinder’s pressure, transfer volume, and transfer speed.

Cylinder number	Size (L)	Pressure <sup>a</sup>		molar fraction <sup>b</sup>		Drift <sup>c</sup> Amount (μmol)	Molar fraction (μmol/mol)	Transfer <sup>d</sup> Speed (L/min)
		Before (MPa)	After (MPa)	Before (μmol/mol)	After (μmol/mol)			
Mother CPC00878	10	9.8	4.4	379.138	379.322	3.15 ± 0.73	0.18	62
Daughter CPC00875	10		4.5		379.034	-1.82 ± 0.74	-0.10	
Mother CPD00092	10	10.5	4.8	458.611	458.715	1.96 ± 0.79	0.10	211
Daughter CPD00093	10		4.4		458.487	-2.12 ± 0.73	-0.12	

Mother	CPD00076	10	4.1	2.0	378.103	378.243	$1.09 \pm 0.33$	0.14	27
Daughter	CPB28688	10		2.0		377.982	$-0.94 \pm 0.33$	-0.12	
Mother	CPD00069	10	13.5	8.0	377.523	377.602	$2.46 \pm 1.32$	0.08	216
Daughter	CPD00072	10		4.5		377.333	$-3.31 \pm 0.74$	-0.19	
Mother	CPD00070	10	13.2	7.8	377.936	378.026	$2.73 \pm 1.29$	0.09	24
Daughter	CPD00074	10		5.1		377.751	$-3.68 \pm 0.84$	-0.19	
Mother	CPB16349	10	8.8	7.0	419.319	419.350	$0.84 \pm 1.16$	0.03	54
Daughter	CPC00484	10		1.7		419.135	$-1.21 \pm 0.28$	-0.19	
Mother	CPD00069	10	6.6	5.6	377.602	377.635	$0.72 \pm 0.93$	0.03	19
Daughter	CPD00072	10		0.8		377.463	$-0.43 \pm 0.13$	-0.14	
Mother	CQB15834	48	14.5	8.6	376.876	376.950	$12.49 \pm 7.18$	0.07	167.7
Daughter	CPD00072	10		8.1		376.780	$-3.01 \pm 1.33$	-0.10	55.2
	CPD00074	10		8.0		376.792	$-2.60 \pm 1.31$	-0.08	54.5
	CPD00073	10		8.5		376.787	$-2.93 \pm 1.40$	-0.09	57.9
Mother	CQB15808	48	13.9	8.5	377.200	377.255	$9.18 \pm 7.10$	0.05	291.6
Daughter	CPD00070	10		8.3		377.127	$-2.34 \pm 1.37$	-0.07	99.6
	CPD00069	10		7.8		377.093	$-3.24 \pm 1.29$	-0.11	93.6
	CPD00076	10		8.2		377.098	$-3.25 \pm 1.36$	-0.10	98.4
Mother	CPB31362	10	4.13	3.3	441.693	441.722	$0.37 \pm 0.54$	0.03	2.8

Daughter	CPB16311	10		0.86		441.641		$-0.17 \pm 0.14$	$-0.05$	
Mother	CPB31362	10	3.2	1.6	406.184	406.223		$0.24 \pm 0.26$	$0.04$	1.1
Daughter	CPB16311	10		1.5		406.179		$-0.03 \pm 0.25$	$-0.004$	
Mother	CPB28912	10	8.5	4.5	419.853	419.908		$0.95 \pm 0.74$	$0.06$	2.2
Daughter	CPB16463	10		4.0		419.801		$-0.82 \pm 0.66$	$-0.05$	

<sup>a</sup> Pressures were measured using the pressure gauge attached the regulator.

<sup>b</sup> CO<sub>2</sub> molar fractions in mother and daughter cylinders were measured after several hours to half of a day of transferring the mixtures. These values have a measurement uncertainty of 0.030 μmol/mol.

<sup>c</sup> The change in the amount of substance ( $n$ ) for CO<sub>2</sub> were computed from the change in the amount of CO<sub>2</sub> molar fraction ( $c_{CO_2}$ ), the cylinder volume ( $V$ ) and pressure ( $p$ ) in the daughter cylinder using the ideal gas law;  $n = c_{CO_2} \times p \times V / (R \times T)$ . Numbers following the symbol  $\pm$  denote the standard uncertainties calculated based on the measurement uncertainty.

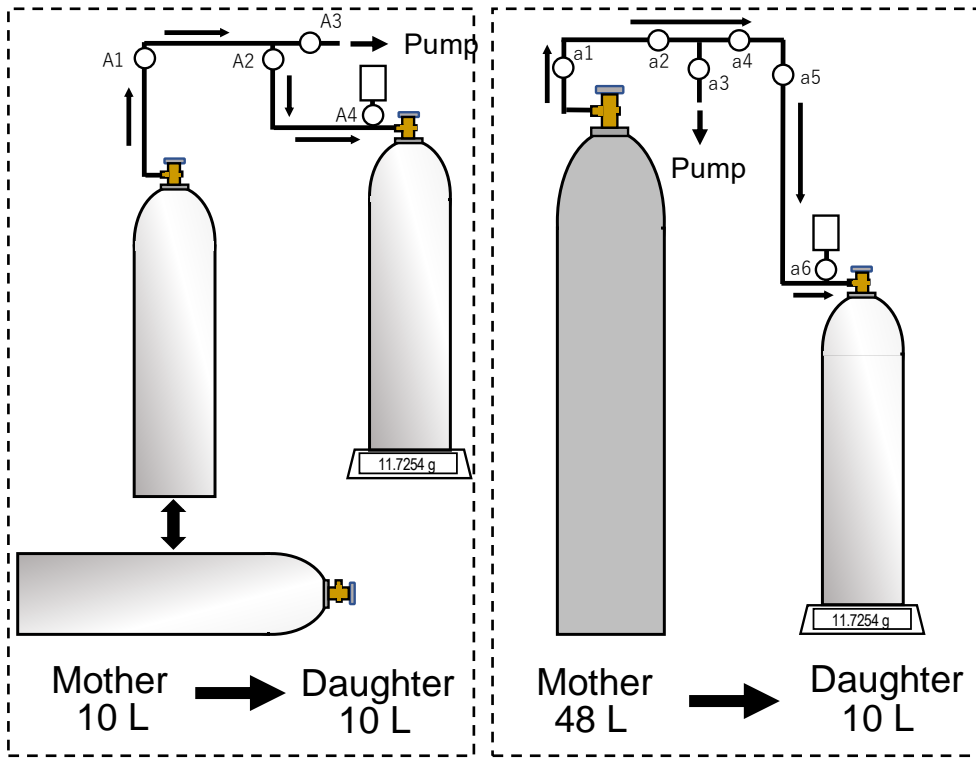
<sup>d</sup> Transfer speeds were roughly computed by dividing transfer volume by transfer time.

625

(a)

630

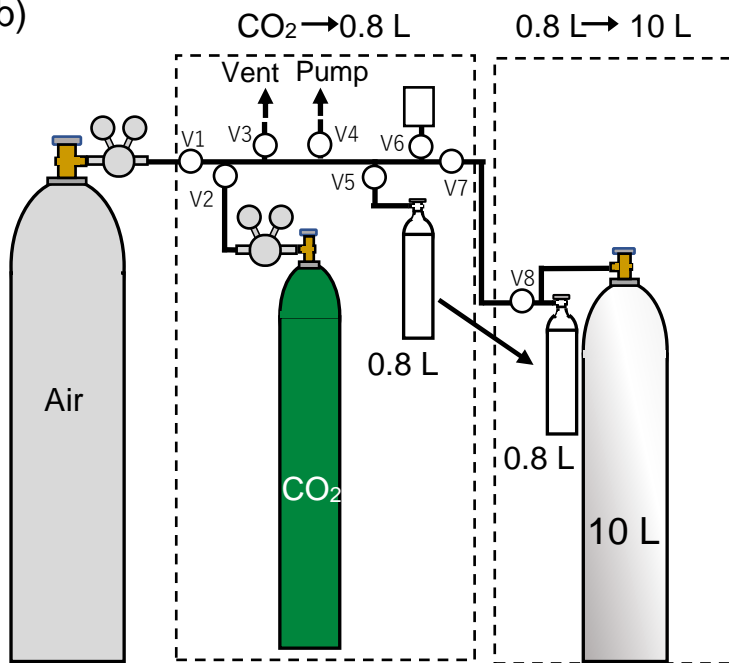
635



(b)

640

645



650

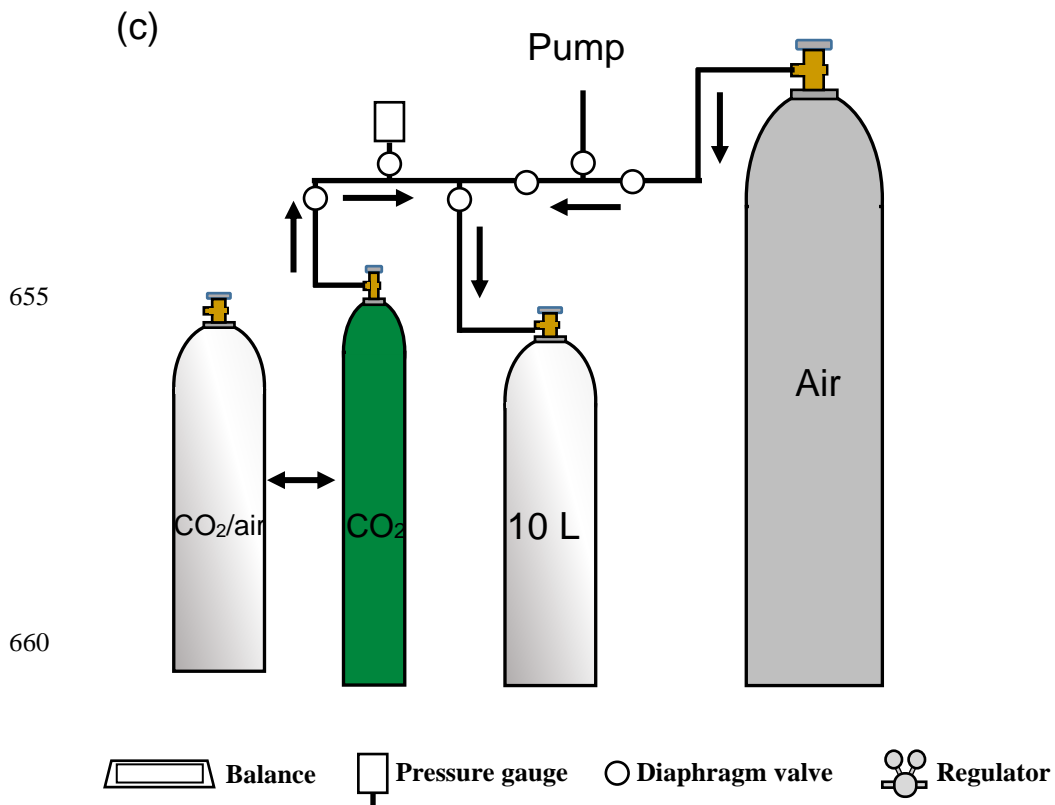


Figure 1 (a) Schematic of the manifold used to transfer a CO<sub>2</sub>/air mixture from a mother cylinder to a daughter cylinder  
 665 in a mother–daughter experiment, (b) the manifold used to transfer pure CO<sub>2</sub> to a 0.8-L aluminum cylinder and from a  
 0.8-L aluminum cylinder to a 10-L aluminum cylinder for preparing a standard mixture via one-step dilution and (c)  
 the manifold used to transfer source gas (pure CO<sub>2</sub> or a CO<sub>2</sub>/air mixture) and dilution gas (purified air).

1  
2  
3  
4  
5  
6  
7  
8  
9  
10  
11  
12  
13  
14  
15  
16  
17  
18  
19  
20  
21  
22  
23  
24

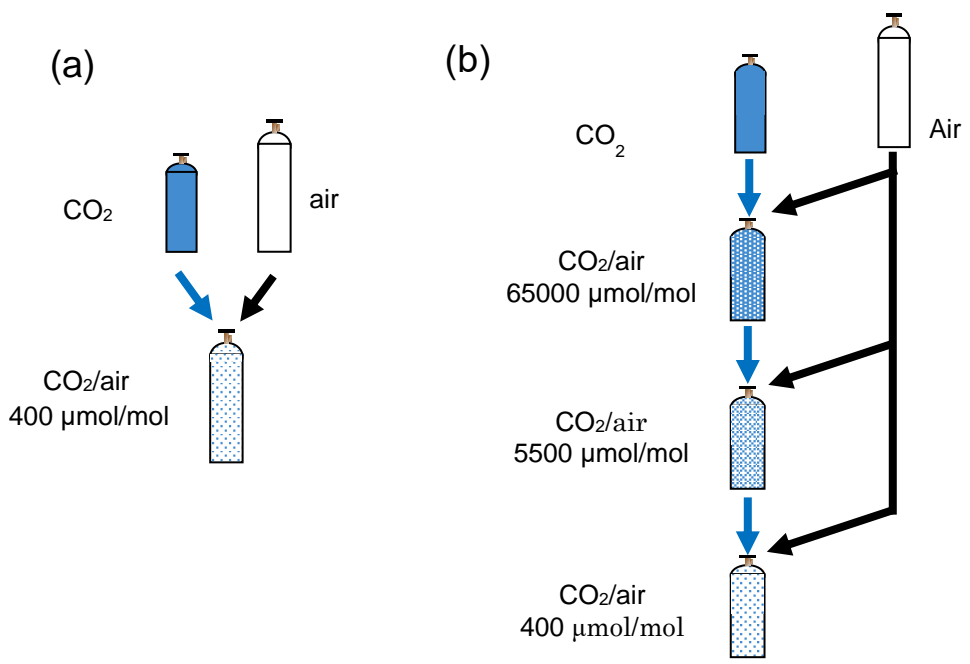
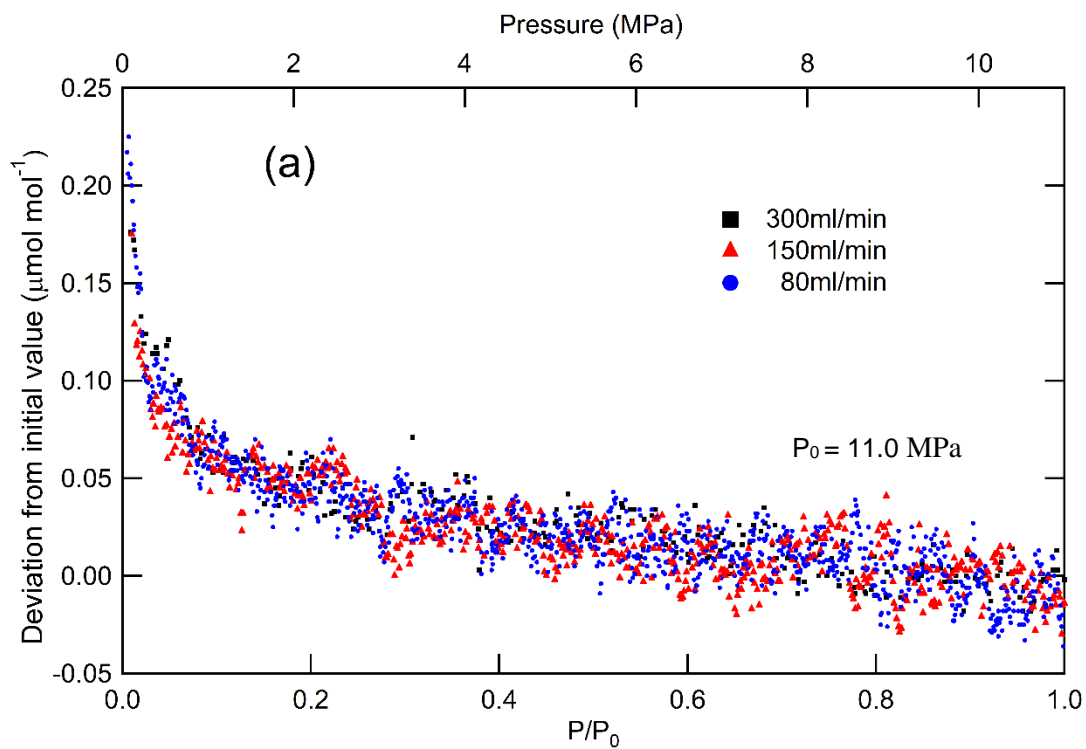
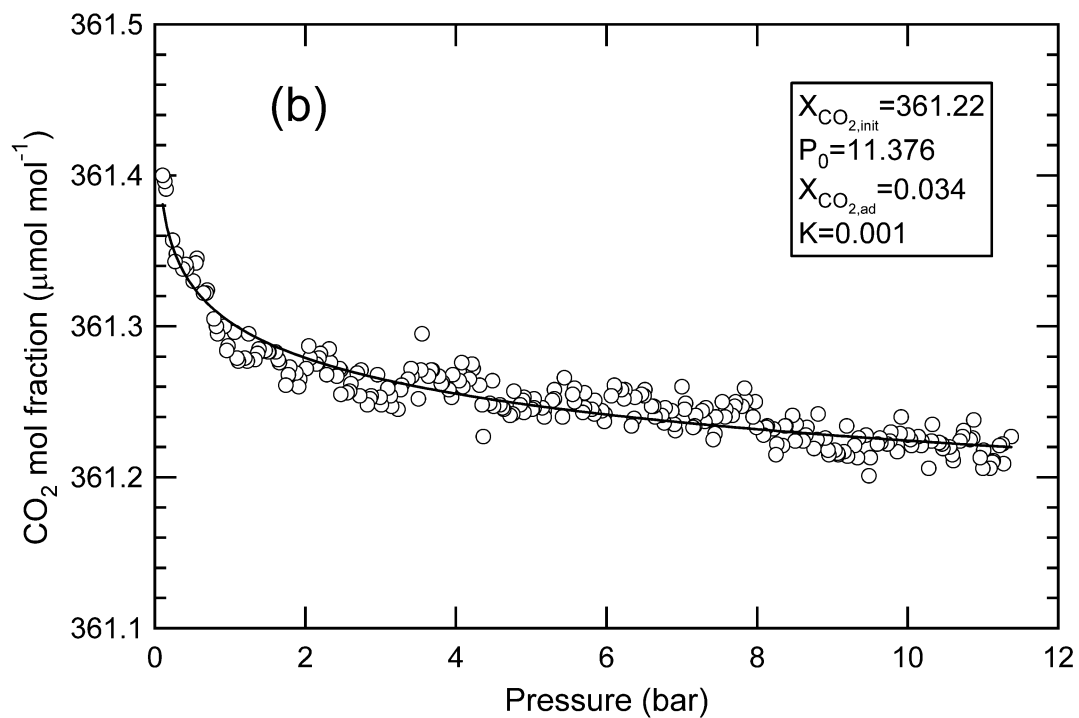


Figure 2 (a) Preparation process of standard mixtures under atmospheric CO<sub>2</sub> level via one-step dilution. (b) Preparation process of 3<sup>rd</sup> gas mixtures under atmospheric CO<sub>2</sub> level via three-step dilutions.

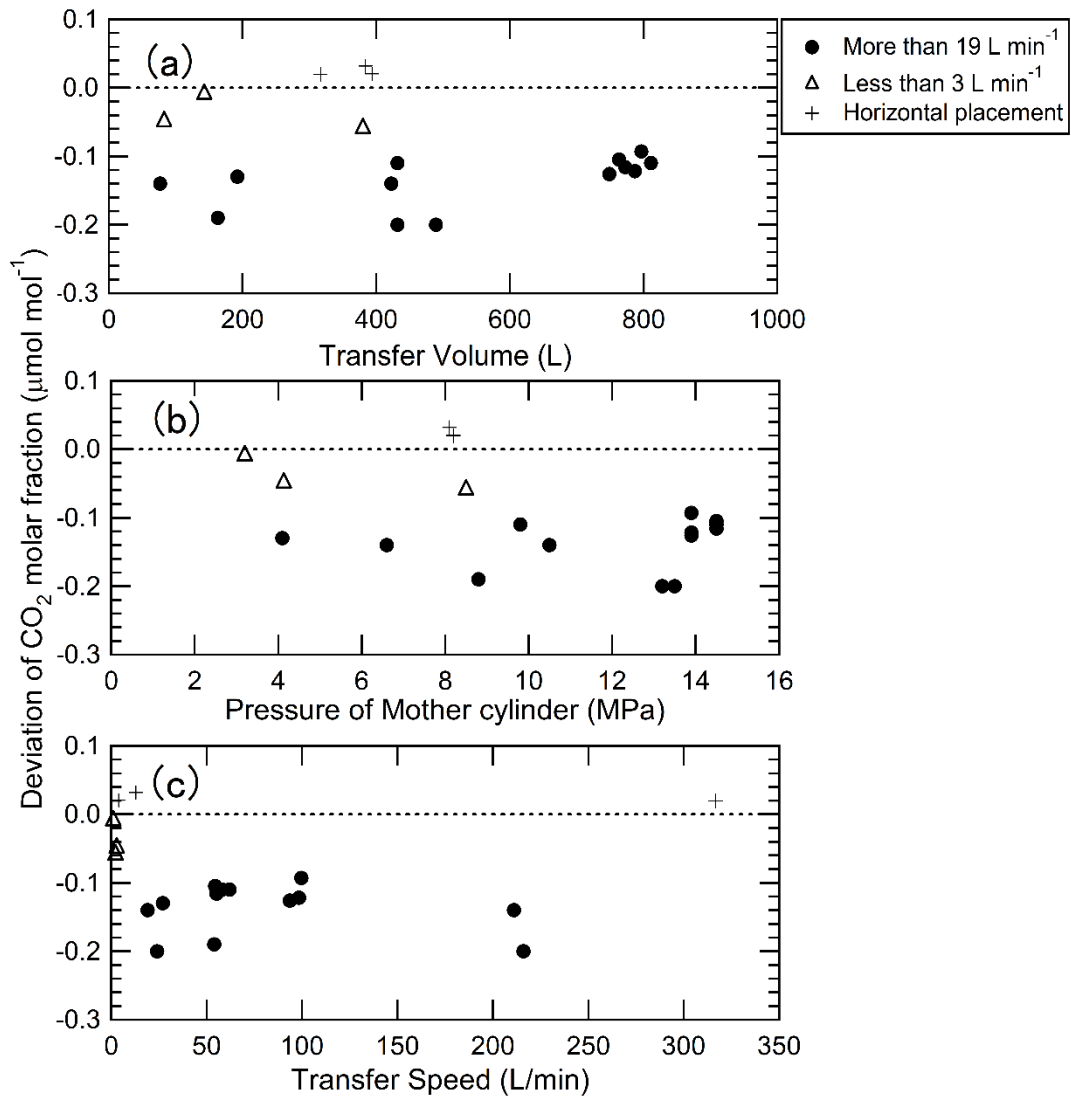


1



2

3 Figure 3 (a) Change of the CO<sub>2</sub> molar fractions from initial value in CO<sub>2</sub>/air mixtures under atmospheric CO<sub>2</sub> level  
 4 against relative pressure as the cylinder was emptied at the flow rates of 80 mL min<sup>-1</sup>, 150 mL min<sup>-1</sup>, and 300 mL  
 5 min<sup>-1</sup> from 11.0 MPa to 0.1 MPa. (b) Typical results obtained by applying the Langmuir model to the change of CO<sub>2</sub>  
 6 molar fractions from initial value in CO<sub>2</sub>/air mixture as the cylinder was emptied from 11.0 MPa to 0.1 MPa.



1

2 Figure 4 Deviations of CO<sub>2</sub> molar fractions in daughter cylinders from initial values against (a) transfer volume (b)

3 mother cylinder's pressure, and (c) transfer speed when the CO<sub>2</sub>/air mixtures under atmospheric level were transferred

4 from the mother cylinder to the daughter cylinder. The closed circles represent the results measured at a transfer speed

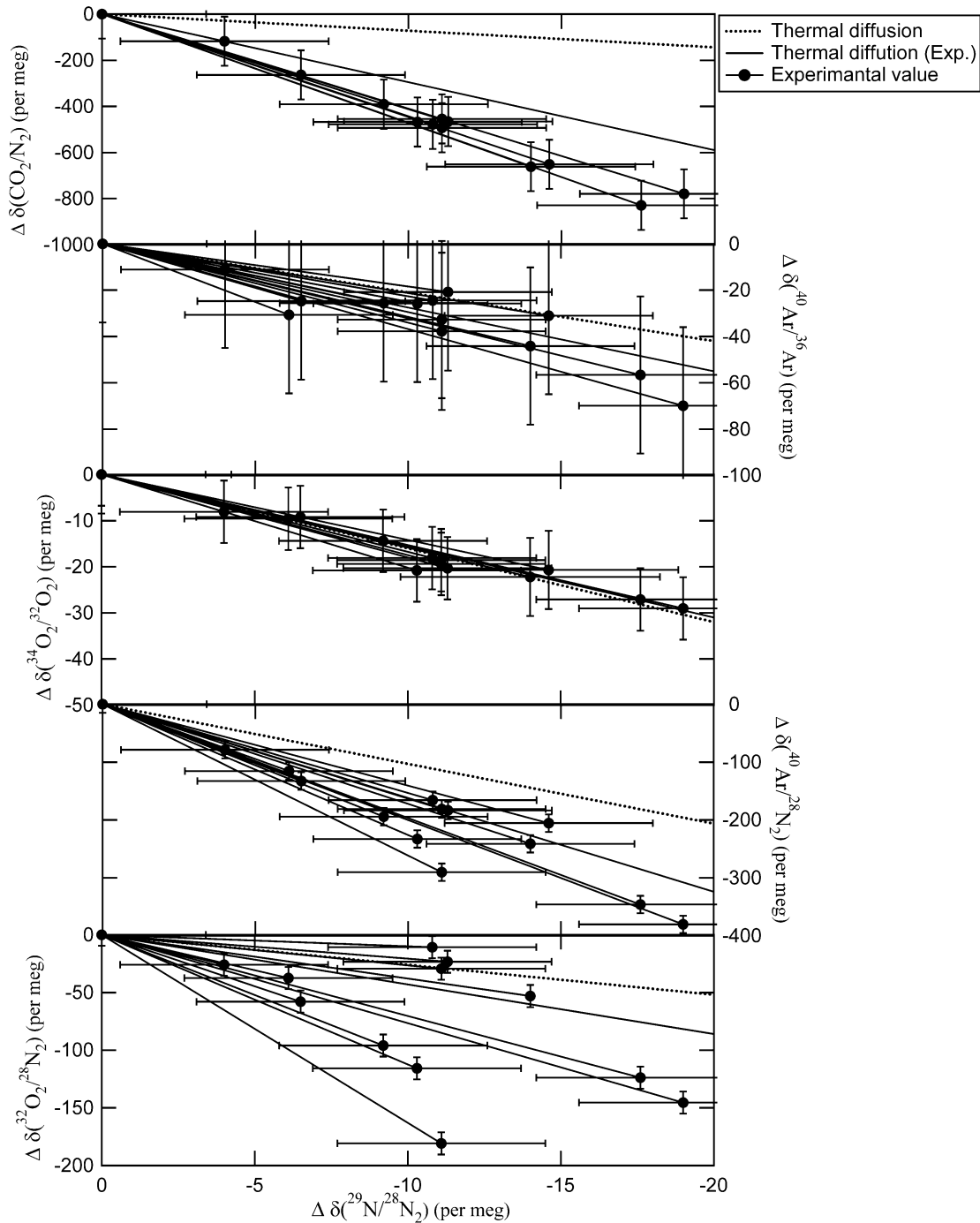
5 of more than 19 L min<sup>-1</sup>, while the open triangles represent the results measured at a transfer speed of less than 3 L

6 min<sup>-1</sup>. These were performed with the vertical mother cylinders plus signs represent the results performed with the

7 horizontal mother cylinders

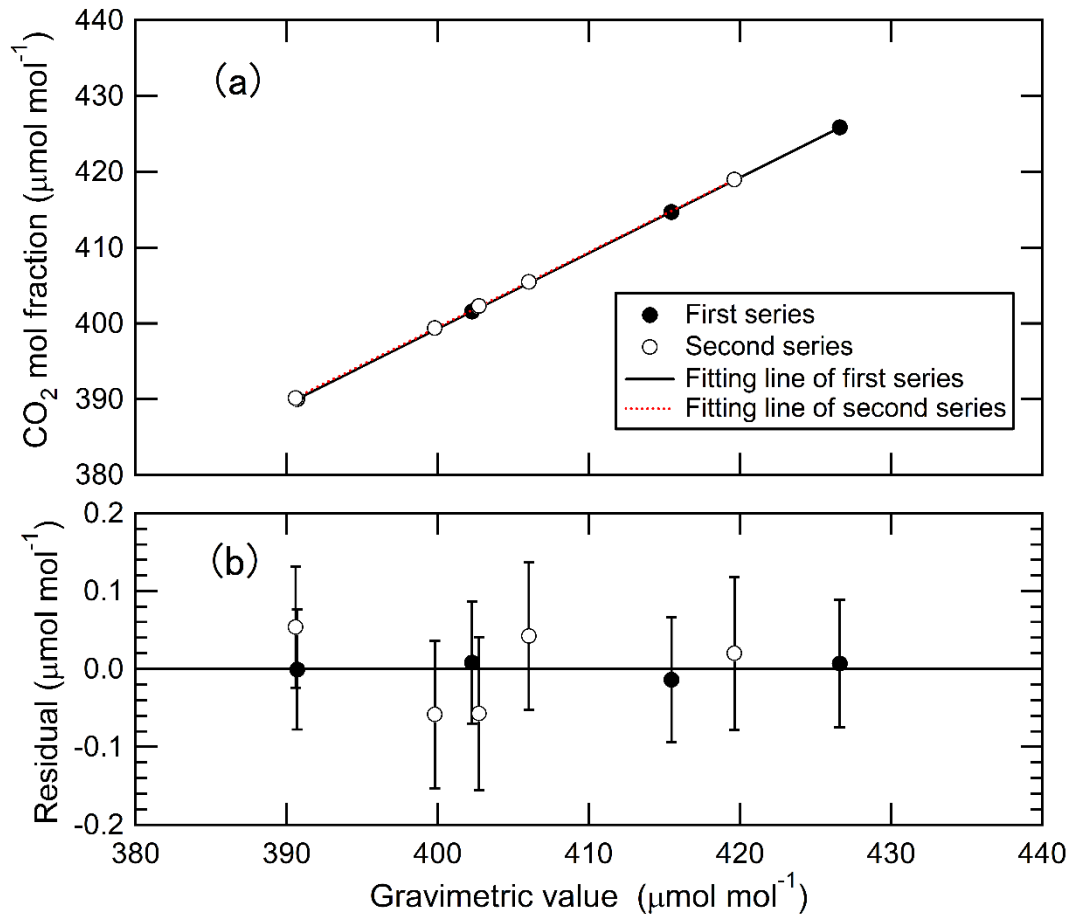
8





1  
2 Figure 5 Relationship between the deviations of  $\delta(^{44}\text{CO}_2/^{28}\text{N}_2)$ ,  $\delta(^{40}\text{Ar}/^{36}\text{Ar})$ ,  $\delta(^{34}\text{O}_2/^{32}\text{O}_2)$ ,  $\delta(^{40}\text{Ar}/^{28}\text{N}_2)$ , and  
3  $\delta(^{32}\text{O}_2/^{28}\text{N}_2)$  with the deviations of  $\delta(^{29}\text{N}_2/^{28}\text{N}_2)$  in the daughter cylinders relative to their mother cylinders after the  
4  $\text{CO}_2/\text{air}$  mixtures under atmospheric level were transferred from the mother cylinder to the daughter cylinder. **Error bar**  
5 **expresses expanded uncertainty of the deviations.** The red dotted line represents the theoretical value of thermal  
6 **diffusion, respectively, (Langenfelds et al. 2005).** The red solid lines represent the deviations due to thermal diffusion,  
7 experimentally estimated by Ishidoya et al. (2013, 2014).

1



2

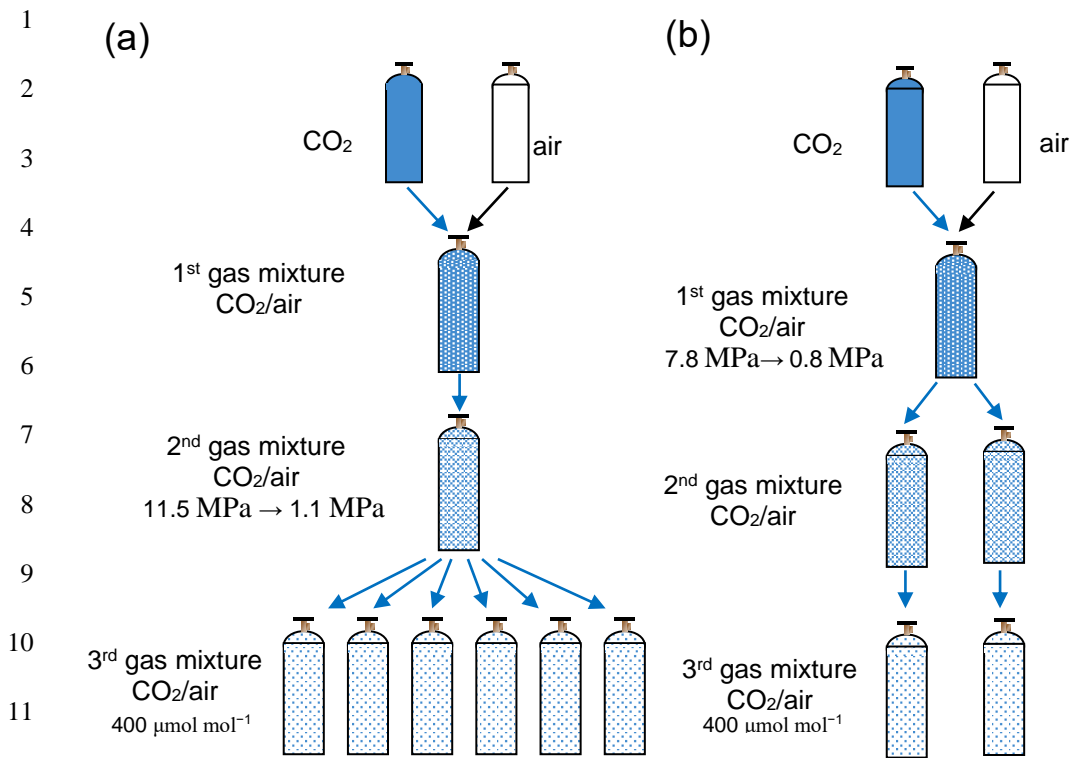
3 Figure 6 (a) Relationships between the measured CO<sub>2</sub> molar fractions and the gravimetric values for two series of  
4 standard mixtures prepared via one-step dilution. (b) Residuals from the Deming least-square fit shown in (a).

5

6

7

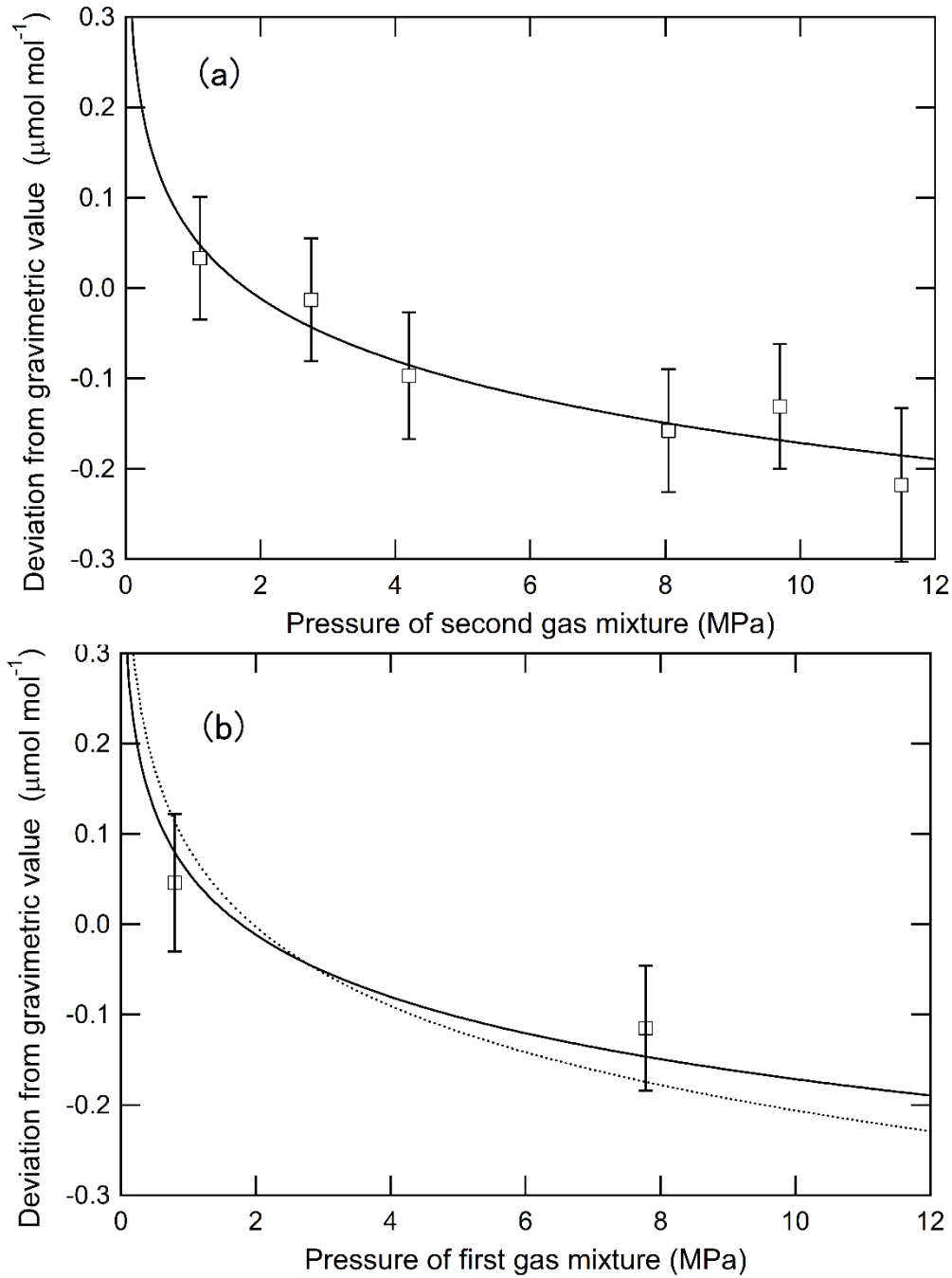
8



19  
20  
21  
22  
23

Figure 7 (a) Preparation process of the 3<sup>rd</sup> gas mixtures under atmospheric CO<sub>2</sub> level via three-step dilutions to evaluate the fractionation in the third step and (b) second step dilutions.

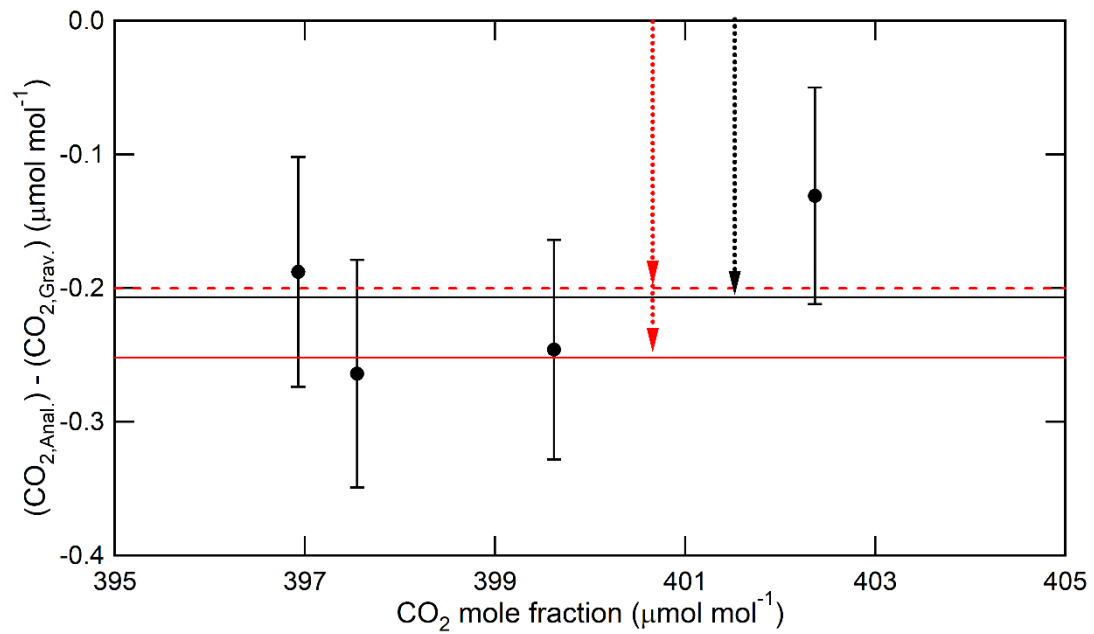
1



2

3 Figure 8 (a) Deviations of the measured  $\text{CO}_2$  molar fractions from the gravimetric values against the pressure of the 2<sup>nd</sup>  
4 gas mixture.  $\text{CO}_2$  molar fractions determined on the basis of the standard mixtures prepared via one-step dilution. The  
5 solid line represents the Rayleigh model fit for the plots. (b) Deviations of the measured  $\text{CO}_2$  molar fractions from the  
6 gravimetric values against the pressure of the 1<sup>st</sup> gas mixture. The  $\text{CO}_2$  molar fractions determined on the basis of the  
7 standard mixtures prepared via one-step dilution. The solid and dotted lines represent the Rayleigh model fit based on  
8 the fractionation factor of  $0.99975 \pm 0.00004$  and  $0.99968 \pm 0.00010$ .

1 Re



2

3 Figure 9 Deviations of the measured values from the gravimetric values of CO<sub>2</sub> molar fractions in the standard mixtures  
4 (3<sup>rd</sup> gas mixtures) prepared via three-step dilutions. The measured values were calculated from the calibration line  
5 obtained by applying the Deming least square fit to the measured data. The black line represents the average value of  
6 the deviations. The red solid and dotted lines represent the values calculated using fractionation factors of  $0.99968 \pm$   
7  $0.00010$  and  $0.99975 \pm 0.00004$ , respectively. The red and black arrows represent the deviation of CO<sub>2</sub> molar fraction  
8 in the 3<sup>rd</sup> gas mixtures according to the fractionation of CO<sub>2</sub> and air.

9